

UNCLASSIFIED

AD NUMBER

AD330247

CLASSIFICATION CHANGES

TO: UNCLASSIFIED

FROM: CONFIDENTIAL

LIMITATION CHANGES

TO:  
Approved for public release; distribution is unlimited.

FROM:  
Distribution authorized to U.S. Gov't. agencies and their contractors;  
Administrative/Operational Use; JUL 1962. Other requests shall be referred to Ordnance Corps (Army), Redstone Arsenal, AL.

AUTHORITY

31 Jul 1964, DoDD 5200.10 ; AOC/RED per DTIC form 55

THIS PAGE IS UNCLASSIFIED

~~UNCLASSIFIED~~

AD 330 247

*Reproduced  
by the*

ARMED SERVICES TECHNICAL INFORMATION AGENCY  
ARLINGTON HALL STATION  
ARLINGTON 12, VIRGINIA



~~UNCLASSIFIED~~

D

NOTICE: When government or other drawings, specifications or other data are used for any purpose other than in connection with a definitely related government procurement operation, the U. S. Government thereby incurs no responsibility, nor any obligation whatsoever; and the fact that the Government may have formulated, furnished, or in any way supplied the said drawings, specifications, or other data is not to be regarded by implication or otherwise as in any manner licensing the holder or any other person or corporation, or conveying any rights or permission to manufacture, use or sell any patented invention that may in any way be related thereto.

CONFIDENTIAL

Report No. S-35

Special

Copy No. 63

July 31, 1962

# ROHM & HAAS COMPANY

REDSTONE ARSENAL RESEARCH DIVISION

HUNTSVILLE, ALABAMA



REPORT NO. S-35

INTERIM REPORT

THE DEVELOPMENT OF PLASTISOL PROPELLANT  
FOR THE NIKE-ZEUS BOOSTER (U)

ASTIA  
RECEIVED  
AUG 3 1962  
RESOLVED  
ASTIA A

ORDNANCE CORPS, DEPARTMENT OF THE ARMY

This document contains information affecting the national defense of the United States within the meaning of the Espionage Laws, Title 18, U. S. C., Sections 793 and 794. The transmission or the revelation of its contents in any manner to an unauthorized person is prohibited by law.

DOWNGRADED AT 3 YEAR INTERVALS:  
DECLASSIFIED AFTER 12 YEARS.  
DOD DIR 5200.10

CONFIDENTIAL

330247

CATALOGED BY ASTIA  
AS AD NO. \_\_\_\_\_

330 247

CONFIDENTIAL

ROHM & HAAS COMPANY

REDSTONE ARSENAL RESEARCH DIVISION  
HUNTSVILLE, ALABAMA

REPORT NO. S-35

INTERIM REPORT

THE DEVELOPMENT OF PLASTISOL PROPELLANT  
FOR THE NIKE-ZEUS BOOSTER

Approved:



Allen R. Deschere  
General Manager

Contributing Staff:

S. E. Anderson  
L. M. Brown  
F. J. Caudle  
J. D. Clem  
H. T. Downing  
M. L. Essick  
R. C. Farmer  
J. S. Foster  
B. J. Gaines  
S. Gratch  
A. J. Ignatowski  
L. Jenkins  
H. L. McGill  
C. O. Metzger  
P. G. Norris  
C. H. Parr  
J. W. Parrott  
W. W. Seaton  
H. M. Shuey  
M. W. Stone  
W. C. Stone  
T. E. Stonecypher  
G. E. Tabor  
C. E. Thies

CONFIDENTIAL

**CONFIDENTIAL**

**TABLE OF CONTENTS**

	<b><u>Page</u></b>
1. Introduction	1
2. Summary and Conclusions	2
3. Discussion	2
3.1 General Requirements	2
3.2 Propellant Formulation Studies and Evaluation	3
3.3 Propellant Processing	9
3.4 Insulation and Liner Development	12
3.5 Small Motor Tests	16
3.6 Calculated Performance of the Full-Scale Booster	26
3.7 Surveillance	27
3.8 Production Techniques	29
3.9 Logistics	30
 <b>Appendix A</b>	
Establishment of Strain Capability of Plastisol Propellants	A-1
Scale Booster Strain Requirements	A-5
Effect of Humidity on Physical Properties of Plastisol Propellant	A-7
 <b>Appendix B</b>	
Methods of Computation for Surveillance Motors	B-1

**CONFIDENTIAL**

CONFIDENTIAL

INTERIM REPORT

THE DEVELOPMENT OF PLASTISOL PROPELLANT  
FOR THE NIKE-ZEUS BOOSTER

1. INTRODUCTION

*An attempt was initiated to develop*

On May 18, 1961, the Redstone Arsenal Research Division of Rohm & Haas Company entered into a contract with the Army Ordnance Missile Command (AOMC) to investigate the use of plastisol nitrocellulose propellant in the Nike-Zeus propulsion system. The objective of this contract, DA-01-021-ORD-12341, was the development of a propulsion system for the Nike-Zeus booster, including the selection of a suitable propellant, propellant configuration, compatible liner system, and ignition system. All testing was to be done in scale motors containing less than 100 lb of propellant. It was recognized that the propellant physical property requirements for the booster would be more severe than those for the other stages because of the high acceleration loads on the long thin star points. Hence, if plastisol could be used satisfactorily in the booster, it could be applied fairly readily to the other stages at a later date.

*to p. 2*

Rohm & Haas Composition 112, which was satisfactorily developed for the Missile A program, was selected for the initial development. In addition, a comprehensive liner study was required to select a compatible liner which would withstand storage and firing over a fairly wide temperature range, and still be reasonably simple to install. The selected propellant and liner system was to be tested in small static test motors and other test configurations to establish the ballistic, physical, and storage characteristics of the propulsion system. Finally a logistic study was required to determine the availability of propellant ingredients.

CONFIDENTIAL

2. SUMMARY AND CONCLUSIONS

Plastisol propellant compositions were evaluated in a 1/5-scale (linear dimensions) Nike-Zeus configuration; at least one composition (178<sub>cf</sub>) gave results equal to or slightly superior to those currently obtained in booster motors loaded with other improved high energy propellants. Production of the 178 propellant is comparatively simple and is very reproducible. Calculations showed that its physical properties are more than adequate (by a factor of 2) for use in the Zeus system. ~~Although no production facilities are in existence to manufacture large quantities of Composition 178, these facilities could be provided, probably within one year, during which time facilities could also be made available to supply all the needed raw materials.~~

Only minor modifications of existing propellant facilities are required to produce plastisol propellants. These modifications are primarily limited to the mixer, which should be of the vertical turbine type, widely used in the chemical industry. Propellant mixing must be considered as a Class 9 hazard operation. Raw materials handling, casting, curing, and inspection facilities may be substantially unchanged from existing operations.

3. DISCUSSION

3.1 General Requirements

One requirement of this contract was to formulate and develop a plastisol nitrocellulose propellant composition for use as a possible back-up to the current Thiokol Chemical Corporation composition. To assure a ready comparison with existing performance data, the booster configuration as designed by Thiokol was selected

with the exception that all work would be done in 1/5-scale size hardware (Fig. 1). The following requirements were specified for the booster motor.

1. The propellant must be useable in the existing motor case with existing mandrels and associated hardware.
2. Burning time should be 4.8 seconds at 77°F.
3. Action time should not exceed 5.3 seconds at 77°F.
4. Propellant burning rate should be 0.73 inches per second at 1000 psi and 77°F.
5. Maximum firing pressure should not exceed 1350 psi ( $P_{\max} + 3\sigma @ 100^\circ\text{F} < 1350 \text{ psi}$ ).
6. Firing temperature range should be 20°F to 100°F.
7. Transportation and cycling temperature range should be -40°F to 120°F.
8. Igloo storage time should be at least five years.
9. Propellant should withstand acceleration loads of 35 g's.
10. The terminal boost velocity should be equal to or greater than that of the high performance booster under development by Thiokol Chemical Corporation.

### 3.2 Propellant Formulation Studies and Evaluation

Plastisol is a castable propellant consisting of plastisol nitrocellulose fluid ball powder plasticized with triethylene glycol dinitrate as a binder and filled with aluminum and ammonium perchlorate as the fuel and oxidizer. The propellant is mixed as a low viscosity slurry, cast into motors, and cured at 105°F.

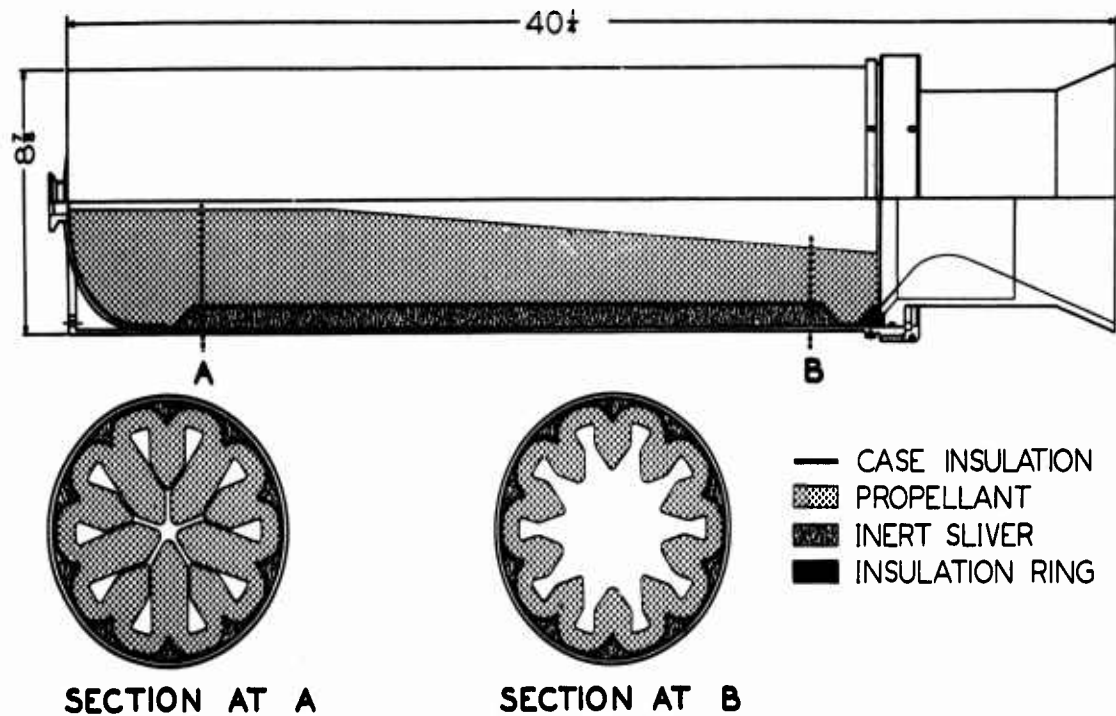


Fig. 1 Nike-Zeus 1/5-scale booster configuration.

To meet the specified requirements, the propellant development program was divided into two phases. The first was an evaluation of Composition 112, which was successfully demonstrated in the Missile A program, and the second was the development of a new formulation based on 112, which would give improved performance by increasing density and specific impulse.

Phase I turned out to be a comparatively straightforward program. The properties of the 112 composition used in the Missile A program were close to those required in the Zeus program. Only a modification of burning rate was required to meet most of the requirements. Based on extensive previous experience with Composition 112, a definite relationship between burning rate and oxidizer particle size had been established (Fig. 2). The oxidizer (ammonium

perchlorate) particle size used in a particular formulation is indicated by the subscript following the composition number (112<sub>cd</sub>). Although the calculated and measured performance of Composition 112 was slightly lower than that required in the Zeus booster application, it was clearly evident that a plastisol composition could be formulated and processed which would meet or exceed the established requirements. The selection of an improved composition was the objective of Phase II.

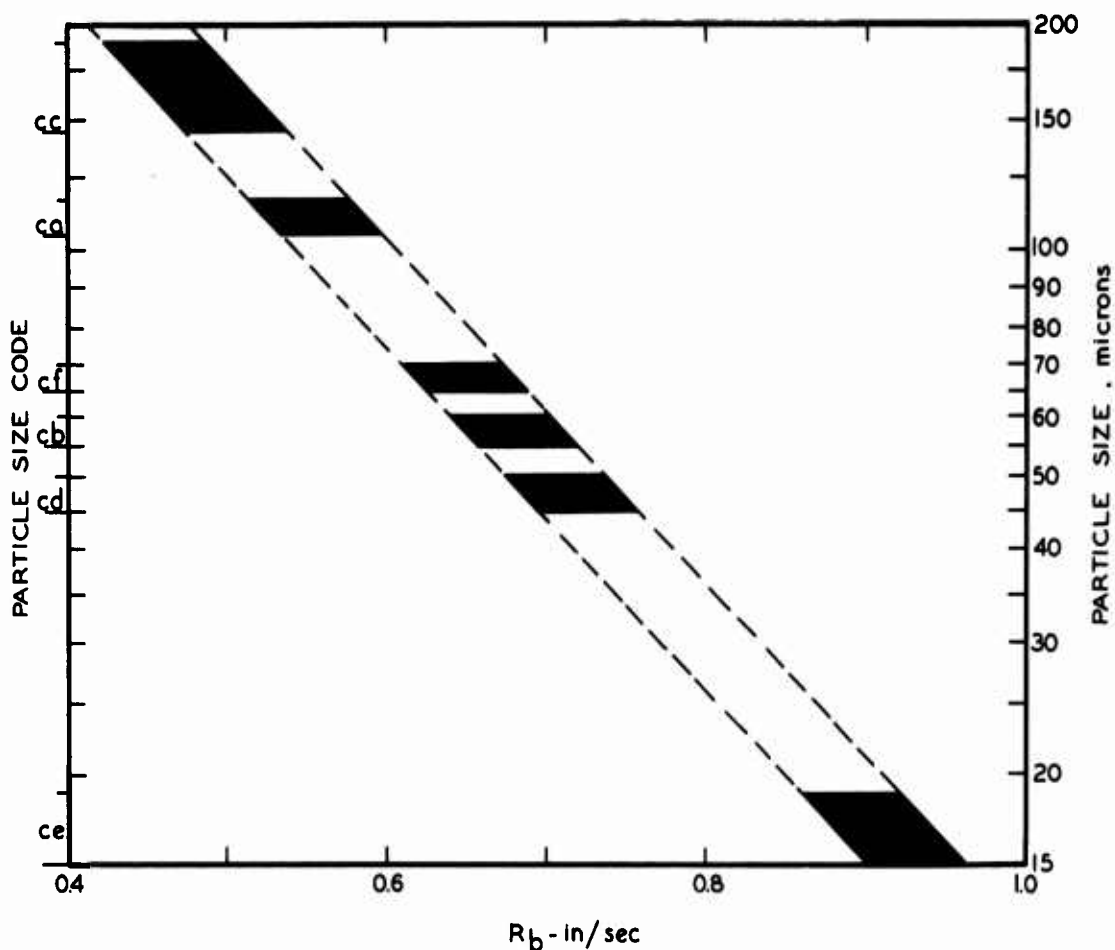


Fig. 2 Burning rate vs. oxidizer particle size in Composition 112 propellant.

An improvement in performance of a plastisol composition could be realized in two ways, either by an increase in specific impulse or by an increase in propellant density, preferably by both. With these objectives in mind, twenty-one compositions were

formulated. These were compared to Composition 112 and to each other on the basis of density, processing viscosity, and physical properties. Of the 15 compositions which were processed for viscosity and physical property evaluation, nine were selected for loading into static test motors and test firing to determine such parameters as burning rate, specific impulse, and volumetric impulse. Volumetric impulse was important because the required propellant configuration fixed the available propellant volume; therefore, it was desirable to maximize this parameter. After extensive testing, three compositions (172, 176, 178) were selected for final evaluation (Table I). All three compositions were better than Composition 112.

Table I  
Comparison of Phase II Plastisol Compositions  
Data Measured in 6C5-11.4 Standard Evaluation Motors

	<u>Composition</u>			
	<u>112</u>	<u>176</u>	<u>177</u>	<u>178</u>
Fluid Ball Powder (Type B)	16.67	9.00	12.84	10.92
Triethylene Glycol Dinitrate	37.33	30.00	33.66	31.83
Ammonium Perchlorate	30.00	37.00	33.50	35.25
Aluminum	15.00	23.00	19.00	21.00
Resorcinol	1.00	1.00	1.00	1.00
Theoretical Density (lb/in <sup>3</sup> )	.0604	.0643	.0623	.0633
Theoretical Specific Impulse Equil. Flow (lbf-sec/lbm)	256.7	263.9	262.6	262.9
Experimental Specific Impulse (lbf-sec/lbm)	245.2	245.7	246.4	247.6
Volumetric Impulse (lbf-sec/cu. in.)	14.81	15.80	15.35	15.67
Temperature Coefficient (%/°F)	0.22	0.16	---	0.21

Although Composition 176 had the highest density impulse, it was only slightly better than Composition 178. At the same time Composition 178 had somewhat better physical properties and specific impulse than 176. On this basis, and the fact that the higher

specific impulse of 178 made it more attractive for possible use in the second and third stages of the Nike-Zeus system, Composition 178 was selected as the best compromise. The specific impulse of Composition 178 was approximately one percent greater than that of Composition 112 (247.6 and 245.2 lbf-sec/lbm), the density was over five percent greater (0.0633 and 0.0604 lb/cu. in.), and the volumetric impulse was almost six percent greater (15.67 and 14.81 lbf-sec/cu. in.). These improvements were realized with no degradation of temperature coefficient or processability and only a slight degradation in physical properties. A comparison of the strain capability of Compositions 112, 176, 177, and 178 is shown in Fig. 3. The curves represent a conservative value of strain capability as described in Appendix A. Pressure vs. K (surface to throat area ratio) and burning rate curves are shown in Fig. 4 for Composition 178<sub>cf</sub> in 1/5-scale Zeus booster motors.

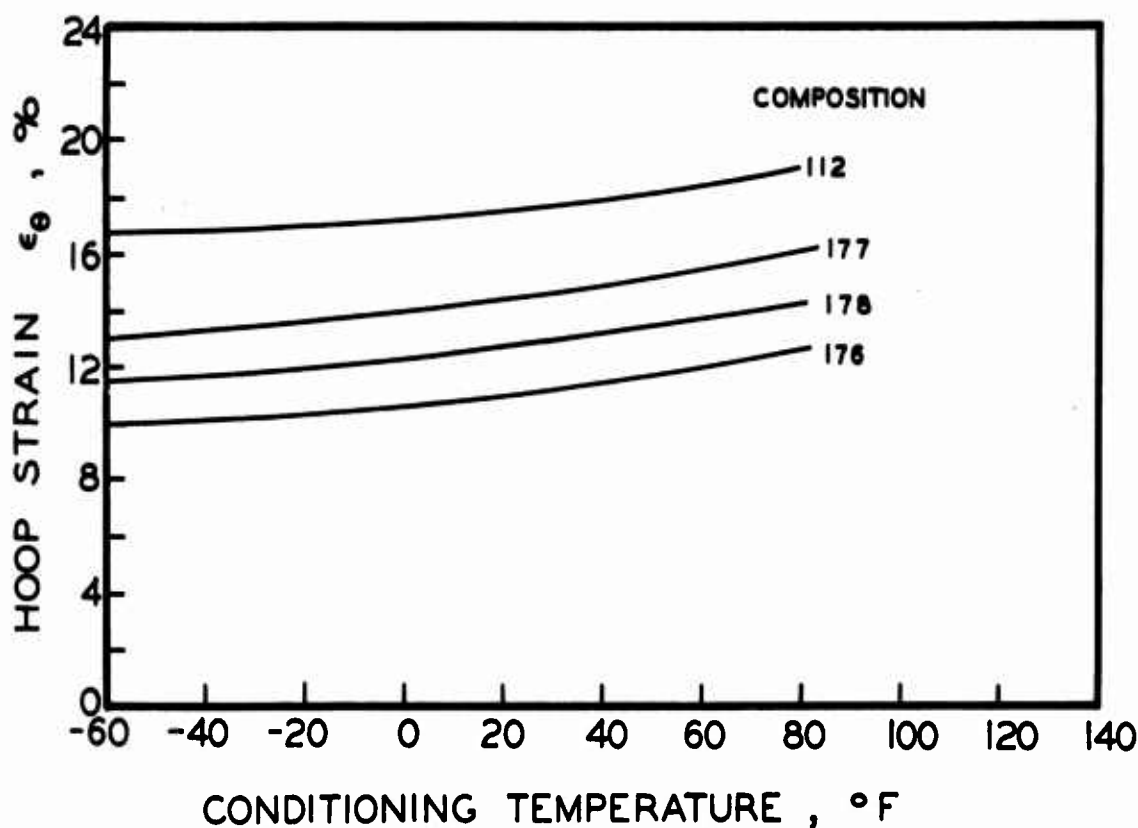


Fig. 3 Strain capability vs. conditioning temperature for various propellant compositions.

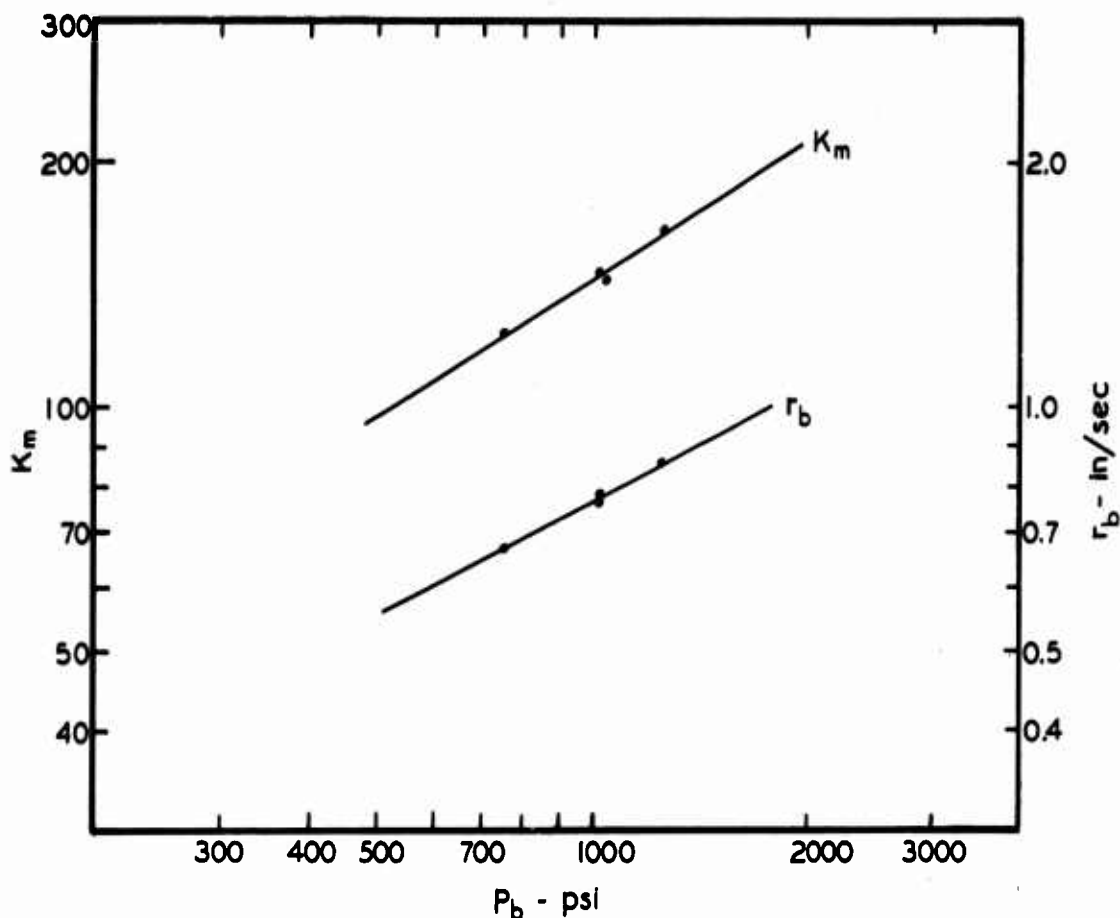


Fig. 4  $P_b$ - $K_m$ - $r_b$  curves for Composition 178<sub>cf</sub>.

Based on the data from Table I, measured data from test firings of plastisol motors, and data from Thiokol<sup>1</sup> and ARGMA<sup>2</sup> test reports on firings with Polysulfide and PBAA propellant, theoretical boost velocities were calculated for four different propellant compositions (Table II). These calculations indicated that Composition 178 would meet the requirements of the contract.

<sup>1</sup>Thiokol Chemical Corporation Report RER-576, February 19, 1960.

<sup>2</sup>ARGMA Test Report TN1E147-16, March 1, 1960.

Table II

Nike-Zeus Booster Velocity Comparison  
(based on present configuration)

<u>Propellant</u>	<u>Ideal Velocity (fps)</u>
Polysulfide	3602
PBAA	3845
Plastisol 112	3750
Plastisol 178	3947

### 3.3 Propellant Processing

Processing of all of the plastisol compositions was relatively simple and straightforward. Extensive processing development on Composition 112 had been done previously for the Missile A program. Only slight variations were required for the successful processing of the other plastisol compositions. Three major objectives were:

1. development of processing information and techniques on Composition 178,
2. control of burning rate through oxidizer particle size control, and
3. production of sufficient high quality motors for testing.

Plastisol propellants have the processing advantages of low viscosity during mixing, low solids concentration, little or no settling under normal processing conditions, and no chemical reaction during processing or curing. To eliminate all settling, the initial viscosity may be controlled by dissolving a small amount of

Ball Powder in the plasticizer (TEGDN) prior to mixing. A flow diagram of the plastisol propellant processing operation is shown in Fig. 5. A flow diagram for loading the rocket motors is shown in Fig. 6.

A quality control program was conducted concurrently with the process development and production stages of the contract. All raw materials (propellant ingredients) were analyzed and checked before use, both for purity of the individual ingredient and in combination in a propellant sample to ensure that the resulting propellant would meet the physical and ballistic requirements. A dilatometric curing test, previously developed by this Division, was used to measure the curing rate and curing shrinkage of a particular combination of nitrocellulose ball powder and TEGDN plasticizer. This test was used to ensure adequate pot life for processing, complete cure in a reasonable time, and low curing shrinkage to minimize stresses in the propellant.

Standard operating procedures were established for mixing, casting and curing. To check the quality of each batch of propellant, physical properties were evaluated and compared with previous data, and each motor was subjected to visual and X-ray inspection. Samples (2-in. cubes) were made with each batch of propellant and were stored at 175°F for at least 45 days to determine the high temperature stability of the propellant. No failures were observed during the production phase of the program. Typical values of propellant properties are presented in Table III.

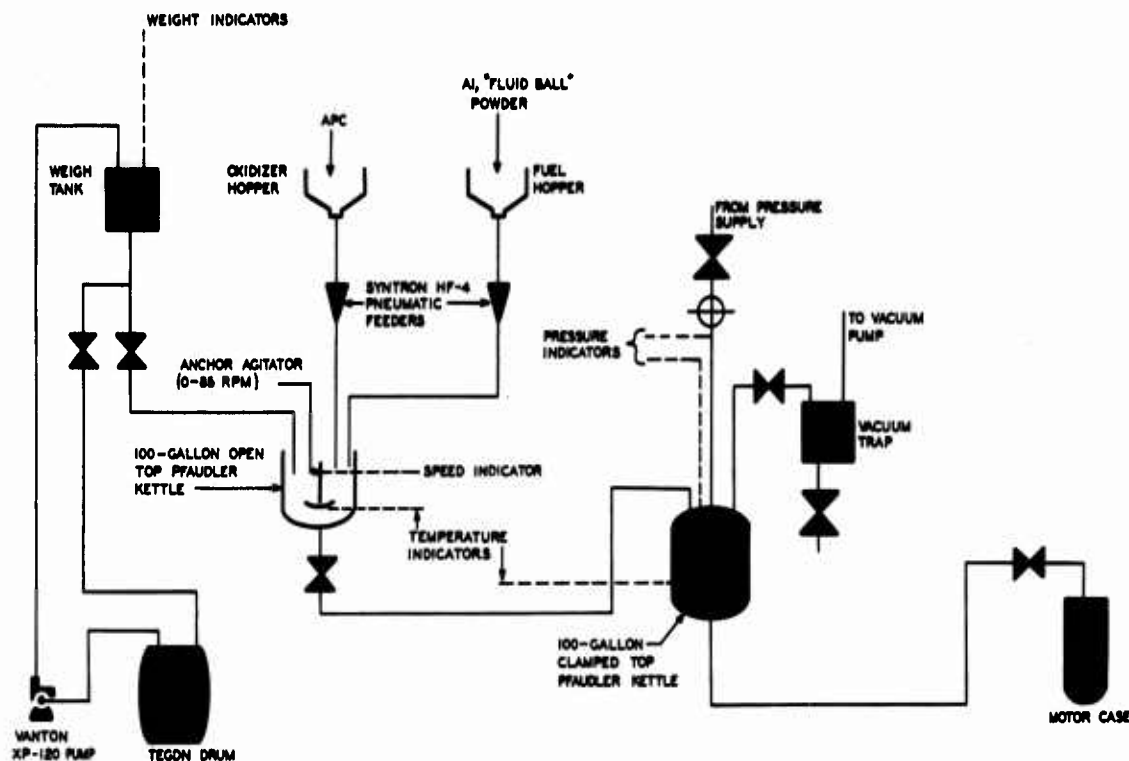


Fig. 5 Flow diagram for Plastisol propellant processing.

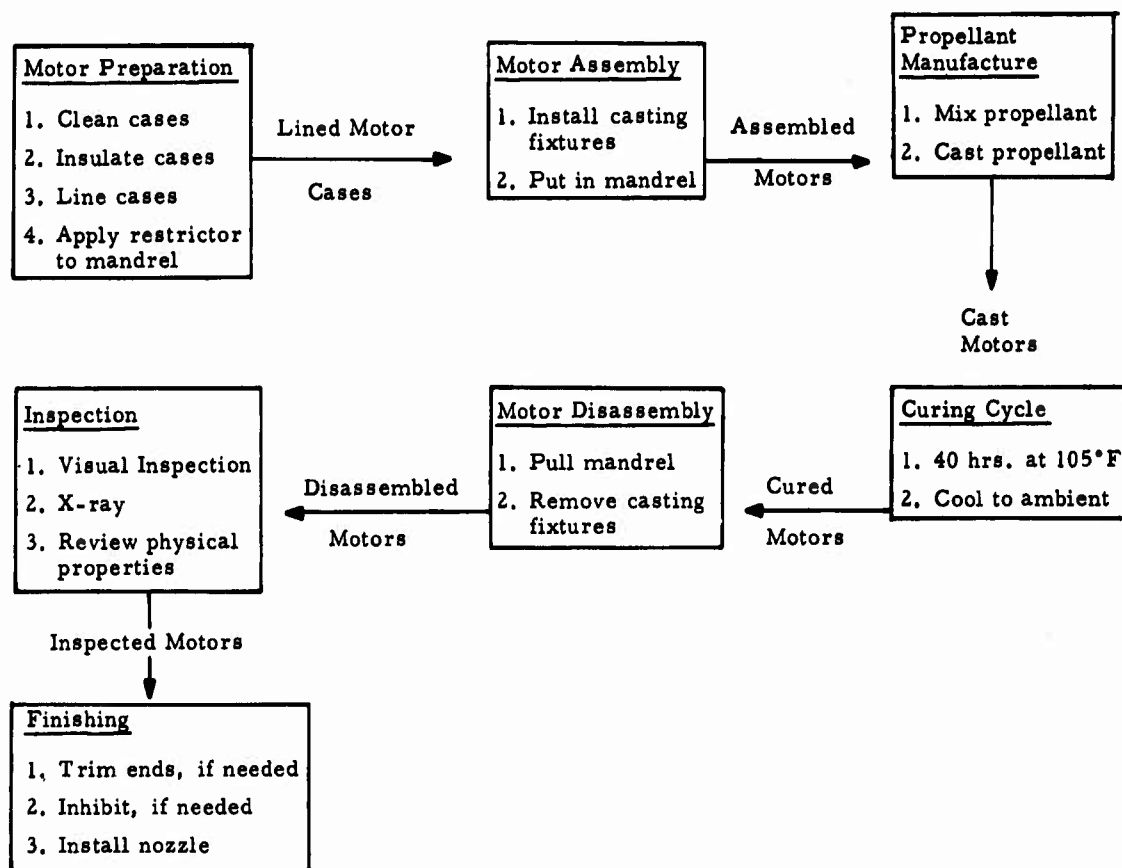


Fig. 6 Flow diagram for preparation and loading of test motors.

Table III

Properties of Plastisol Composition 178<sub>cf</sub>

Density, lb/cu. in.	0.063
Tensile strength @ 77°F, psi <sup>1</sup>	46.7
Elongation @ 77°F, % <sup>2</sup>	13.8
Viscosity, uncured, centipoise	12000-15000
Burning rate @ 1000 psi, in/sec <sup>3</sup>	0.716
Specific impulse, corrected, F° <sub>1000</sub> lbf-sec/lbm <sup>3</sup>	248.3

<sup>1</sup>Maximum engineering stress @ 77°F, Rohm & Haas No. 2 test specimen, cross-head speed 2 inches/minute.

<sup>2</sup>Strain at maximum engineering stress @ 77°F, Rohm & Haas No. 2 test specimen - cross-head speed 2 inches/minute.

<sup>3</sup>Based on firings in 8.5AS31 motors and geometric web-not measured web.

### 3.4 Insulation and Liner Development

The propellant configuration of the Nike-Zeus booster required the use of ten preformed inert slivers equally spaced around the inner wall of the motor to provide a sharp end of burning. A layer of heat insulation was needed to protect the metal case at the domed forward closure and the exposed area between the slivers. A bonding liner was required between the propellant and heat insulation.

The slivers were made of a low density plastic (phenolic micro-balloons in an epoxy binder), as used in the full-scale booster. Extruded aluminum slivers were used in the initial testing until the plastic slivers were available. A mechanical device was designed and built to position the slivers within the motor and to hold them in

place while being bonded with an adhesive of Epon 828<sup>1</sup> and asbestos. This adhesive was selected because of its excellent bonding qualities and its thermal resistance. Other adhesives were investigated, including Epi-Rez 504/Epi-Cure 855<sup>2</sup> with asbestos powder. Although this material also produced an excellent bond, it could not tolerate the temperature required for curing the insulating liner.

Several insulation-liner systems were considered for the booster motor, including rubber-based or reinforced phenolic insulation coated with either epoxy-based or cellulose acetate - based bonding liners. The systems were evaluated with respect to propellant bonding, long term aging, strain requirements, installation problems, low temperature performance, insulation capability, and compatibility with the propellant.

Best results were obtained with an insulating liner formed from 42-RPD<sup>3</sup> phenolic-asbestos mats, bag molded over the entire inner surface of the test motor, including the slivers. A thickness of approximately 0.02 inches was used on the cylindrical surface and a thickness of approximately 0.05 was used in the forward closure. The insulation mats, designated Type 9610, contained 40-45% resin with 20-26% flow. The rubber bags, obtained from Stoner Rubber Company<sup>4</sup>, were separated from the 42-RPD by a thin Teflon release

---

<sup>1</sup>Shell Chemical Company, Cleveland, Ohio.

<sup>2</sup>Jones-Dabney Company, Louisville, Kentucky.

<sup>3</sup>Raybestos-Manhattan Company, Manheim, Pennsylvania.

<sup>4</sup>Stoner Rubber Company, Anaheim, California.

sheet to prevent adhesion of the bags to the insulation. After curing the insulation for two hours at 300 psi and 300°F, the motors were cooled and the insulation surface was grit blasted and vapor degreased to prepare it for the PL-1 bonding liner (Table IV).

Table IV

Composition of PL-1 Bonding Liner

<u>Ingredient</u>	<u>Wt. Percent</u>
Cellulose Acetate	48.4
Triphenyl phosphate	30.5
Santicizer M-17 <sup>1</sup>	18.4
Toluene Diisocyanate	2.4 ml/100g dry ingredient
Red lead	0.24 ml/100g dry ingredient
Acetone	6.5 ml/100g dry ingredient
Methyl cellosolve acetate	484 ml/100g dry ingredient

<sup>1</sup>Monsanto Chemical Company, St. Louis, Missouri.

A 0.002-inch layer of PL-1 bonding liner was sprayed over the entire inner surface of the insulated motor. The selection of the 42-RPD/PL-1 liner system was greatly influenced by the successful use of this system in the Missile A program. Missile A booster motors containing this liner system and Composition 112 propellant have been stored at ambient conditions for over a year with no indication of degradation of the propellant, liner, or bond. Case bond jigs and evaluation cylinders, using this same insulation-liner system, have successfully withstood over eight-months storage at 135°F.

Tensile and shear tests between the steel case and 42-RPD insulation were conducted to ensure that adequate bonding was being obtained and to ensure that the bond would be adequate over a wide temperature range. The test results are shown in Table V.

Table V

Physical Properties of 42-RPD and Bond  
of 42-RPD to Steel

Temperature	Bond Shear Strength psi	Max. Tensile Stress of 42-RPD psi	Max. Strain of 42-RPD %
140	1268	28,600	2.1
77	1228	28,100	2.0
40	1200		
0	1306		
-40	1196	21,300	2.3

An insulation strain requirement of 0.6% had been calculated for use in the booster. The capability is more than three times this value at all test temperatures.

Since the physical properties of the insulation-liner system appeared adequate, the only other problem was a question of compatibility of the sliver or insulation, with the propellant. To determine the effect of these materials on the propellant, 1% of each inert ingredient was mixed into a separate sample of 112<sub>cb</sub> propellant. Taliani tests of each combination showed no effect of any of the inert ingredients (Table VI).

Table VI

Taliani Tests of Propellant with Inert Materials

<u>Sample</u>	<u>Time to 20 mm min.</u>	<u>Slope at 20 mm mm/min.</u>
Propellant, 112 <sub>cb</sub>	73	0.3
Propellant + 1% 42-RPD	67	0.3
Propellant + 1% Microballoon	73	0.3

The insulation-liner system performed adequately in over forty motors fired at various temperatures and after temperature cycling. Char depths were approximately 0.030 inches in the dome section and 0.005 inches in the cylindrical portion, indicating that the insulation thickness is adequate. Estimated insulation thicknesses for the full-scale booster are 0.100 inch in the head end and 0.060 inches in the cylindrical portion. Test firing experience may permit a reduction in these values.

### 3.5 Small Motor Tests

Nearly all tests were conducted in two basic types of test motors: a 6C5-11.4 (propellant 6-in. O.D. x 5-in. I.D. x 11.4-in. long), containing approximately six pounds of propellant, and an 8.5AS31, 1/5-scale Nike-Zeus booster motor, containing approximately 78 pounds of propellant. The 6C5-11.4 static test motors were used for initial ballistic tests to select the propellant composition, determine the burning rate, and evaluate the ballistic parameters of the selected propellant. The selected propellant composition was then tested extensively in the 8.5AS31 (1/5-scale) motor to evaluate the propellant in the Zeus booster configuration. The 6C5-11.4 motors were also used for batch check motors and were cast with each batch of propellant to monitor burning rate and specific impulse.

Initial tests with the 1/5-scale charge configuration were conducted in 5KS4500<sup>1</sup> motor cases, using Composition 112 propellant and 50-gram jelly roll igniters. All of the first three test firings resulted in excessive pressures and considerable propellant breakup. A small pyrogen igniter (2 x 7.5 pipe motor) was used in the next test with the same results after a two-second ignition delay.

The type of ignition had a strong effect on ballistic performance. Propellant breakup occurred each time the jelly roll igniter was used. Various size pyrogen igniters were tested with variable results. By increasing the size of the pyrogen, excessive ignition delays and subsequent propellant breakup were eliminated. The first of the larger pyrogens was made from a 2 x 14 pipe motor and contained Composition 178 propellant. Since satisfactory ignition was also readily obtained with propellant composition 163 in a 2 x 11 pipe motor, this igniter was selected for all demonstration firings.

The pyrogen motor was located in the nozzle of the 1/5-scale motor such that the free area around the nozzle and pyrogen was slightly larger than the throat area. The pyrogen exhaust into the 1/5-scale motor produced a pressure level of about 100 psi until main motor ignition. Main motor ignition was considered to have started at 300 psi for burning time measurements. Pressure rise time from 300 psi to maximum was quite reproducible in all firings. Since pyrogen ignition does not scale linearly, no further attempt was made to optimize the ignition phase, because ignition was already adequate

---

<sup>1</sup>SPIA Jato Manual, Unit 211.

to determine the other ballistic parameters. By extrapolation, ignition of a full-scale plastisol loaded booster should be adequate with the current pyrogen as used in full-scale tests.

By the time the igniter selection was made, Composition 178 had been selected as the propellant, and the 8.5AS31 motors had been received from the manufacturer.

Although no breakup occurred in the next several firings, the initial pressure (immediately after ignition) was excessive, reaching a peak of 150% of the equilibrium pressure. Examination of motors after firing showed that the forward portion of the propellant was burning faster than the rest of the propellant. A variation in pressure across the head end of the complex booster grain was considered a possible cause for the difference in burning rate in the front and back parts of the charge. Coring the center portion of the propellant to provide a larger port area reduced the pressure peak, but the cost in lost propellant was excessive. Finally, various areas in the head end grain perforation were coated with a slower burning restrictor (Table VII) and a pattern chosen, resulting in a pressure trace with no excessive initial pressure peak.

Table VII

Composition of PR-46 Restrictor

<u>Ingredient</u>	<u>Weight %</u>
TEGDN	43
Ball Powder	55
Cab-O-Sil	2

PR-46 was used throughout the rest of the program. The restrictor was painted onto the star points of the front 10-inches of the mandrel to a thickness of approximately 1/16-inch and cured for a day (Fig. 7). After casting and during cure, the propellant and restrictor bonded, so that when the mandrel was withdrawn the restrictor remained on the propellant. The performance of the rounds appeared relatively insensitive to minor variations in the amount of restrictor applied. The weight of restrictor was varied from 170 to 300 grams with no measurable difference in performance.

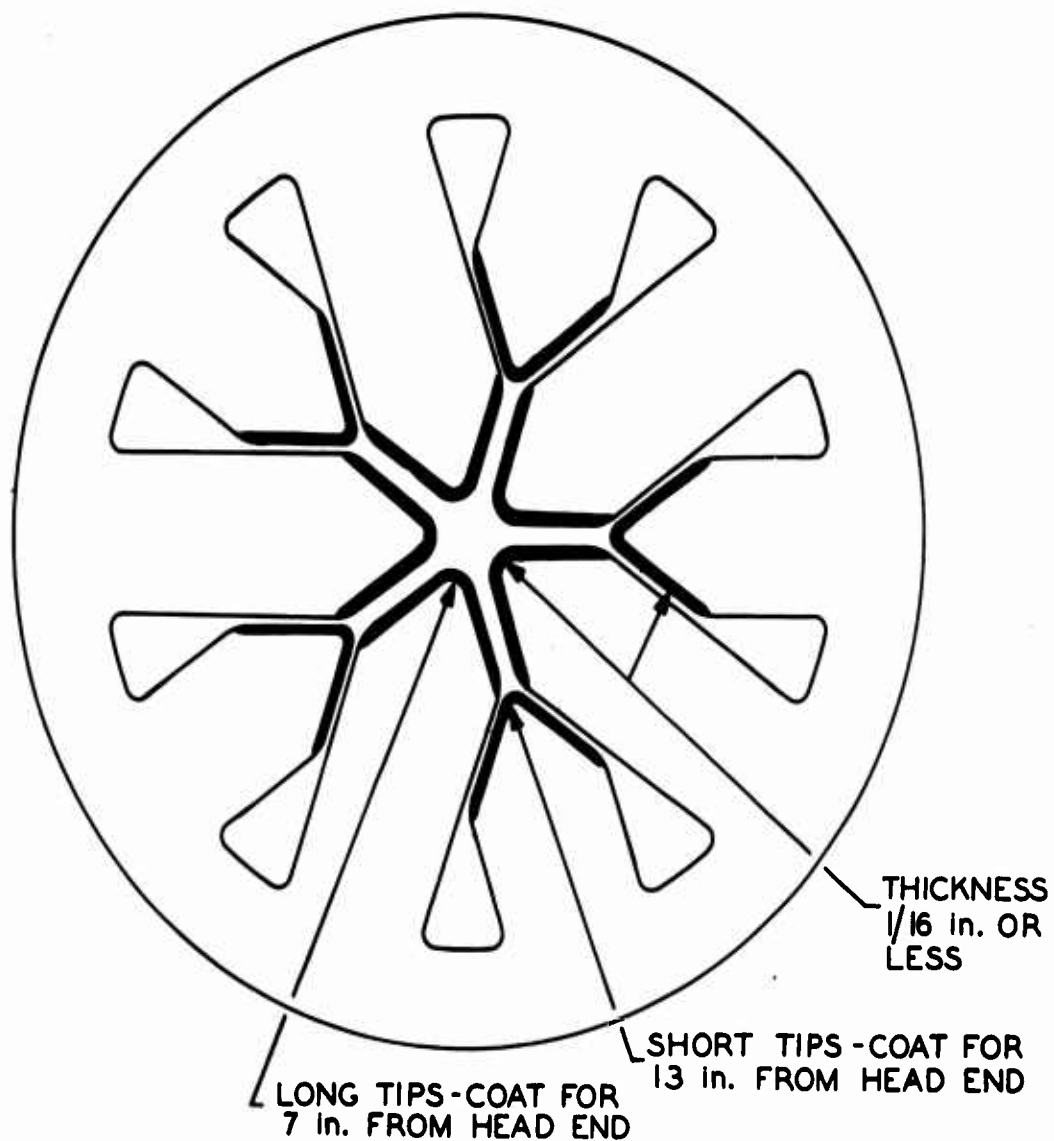


Fig. 7 Restrictor pattern in 1/5-scale Zeus charge.

To determine whether the pressure peak was a function of propellant or scale, a 1/5-scale motor was loaded with a polysulfide propellant by Thiokol Chemical Corporation from the same batch which was being used to load a full-scale booster. Although not as prominent, the pressure peak was present in the 1/5-scale polysulfide motor, indicating that the pressure peak is at least partially a function of scale. Table VIII shows the comparison between the 1/5- and full-scale firings with polysulfide propellant. The data on the full-scale motor are the averages of eight firings reported in Thiokol Chemical Corporation report RER-576 dated February 19, 1960. A comparison of the pressure-time traces of the average full-scale booster and the plastisol loaded 1/5-scale booster is shown in Fig. 8.

Table VIII

Comparison of 1/5 and Full-Scale Firings  
with Polysulfide Propellant

Scale	Burning Rate in./sec	$P_{\max}$	$\bar{P}_b$ psi	$P_{\max}/\bar{P}_b$	Delivered Specific Impulse lbf-sec/lbm
Full	0.73	1160	975	1.19	216.9
1/5	0.72	1208	940	1.29	214.0

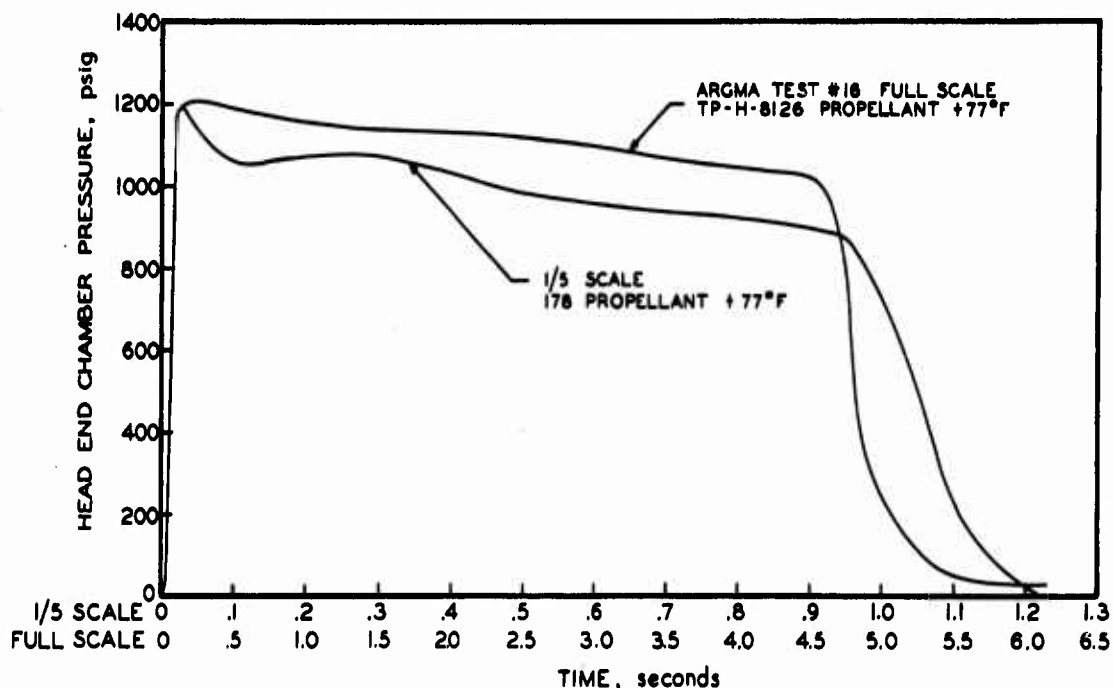


Fig. 8 Pressure-time traces of 1/5 and full scale Zeus boosters.

The preliminary ballistic evaluation of Composition 178 was carried out in twenty-four 1/5-scale firings from 18 batches of propellant. These firings were used to correct the pressure peak problem and to confirm the burning rate established in the 6C5-11.4 test motors. Upon completion of the preliminary evaluation, 39 additional 1/5-scale motors were loaded from six batches of Composition 178<sub>cf</sub> propellant to demonstrate the performance of the Zeus configuration at various temperatures and after temperature cycling. Ballistic data on the temperature conditioned rounds are shown in Tables IX and X.

Table IX  
Results of Firings of 8.5AS31 Temperature Conditioned Motors<sup>3</sup>  
Propellant Composition 178<sub>cf</sub>

Temperature °F	No. Motors	P <sub>max</sub> psig	P <sub>b</sub> psig	P <sub>max</sub> /P <sub>b</sub>	t <sub>b</sub> msec	t <sub>a</sub> msec	r <sub>b</sub> <sup>1</sup> in/sec	I <sub>m</sub> lbf-sec/lbm	F <sub>1000</sub> <sup>2</sup> lbf-sec/lbm	∫ F dt lbf-sec
+77	10	1194	981	1.22	978	1167	.716	232.9	248.3	18,240
	σ	28	15	.04	14	28	.010	0.4	0.6	160
+100	6	1306	1050	1.24	902	1101	.777	232.5	247.2	18,200
	σ	12	21	.02	16	15	.014	0.7	0.7	160
+20	6	1034	861	1.20	1120	1311	.627	231.1	247.8	18,090
	σ	37	26	.02	22	42	.012	1.0	1.0	220

<sup>1</sup>Based on geometric web-not measured web.

<sup>2</sup>Corrected to 1000 psig chamber pressure, 14.7 psia ambient pressure, 0° exit angle, and optimum expansion.

<sup>3</sup>Detailed data on individual rounds are given in Table X.

Table X  
Detailed Data of 8.5AS31 Motors After Temperature Conditioning  
Propellant Composition 178<sub>cf</sub>

Round	Temp. °F	Comments	P <sub>max</sub> psig	P <sub>b</sub> psig	P <sub>max</sub> /P <sub>b</sub>	t <sub>b</sub> msec	t <sub>a</sub> msec	r <sub>b</sub> in/sec	I <sub>m</sub> lbf-sec/lbm	F <sub>b</sub> <sup>1000</sup> lbf-sec/lbm	∫ F dt lbf-sec	∫ F <sub>b</sub> dt / ∫ P <sub>tot</sub> dt
15514	77	Restriction 1" Short	1192	993	1.20	963	1153	.727	232.8	248.1	18290	.90
15515	77	Restriction 1" Short	1168	1001	1.17	959	1125	.730	232.4	247.6	18020	.91
15624	77		1195	982	1.22	992	1182	.706	233.2	248.0	18410	.91
15625	77		1184	988	1.20	979	1165	.715	232.3	247.6	18250	.92
15720	77	Restrictor Failure	1348*	988	1.34*	972	1117	.720	232.8	248.0	17900	.93
15722	77		1235	993	1.24	967	1179	.724	232.4	247.8	18350	.91
15818	77		1242	955	1.30	989	1195	.708	233.6	249.4	18300	.90
15819	77		1174	959	1.22	1005	1200	.696	233.5	249.3	18290	.91
15823	77		1192	977	1.22	980	1171	.714	233.0	248.4	18220	.91
15824	77		1161	974	1.19	977	1186	.716	233.1	248.6	18350	.90
		Average	1194	981	1.22	978	1167	.716	232.9	248.3	18240	.91
		*not included in average										
15626	100		1296	1058	1.22	898	1092	.780	231.9	246.6	18350	.89
15627	100		1320	1060	1.24	899	1110	.780	232.4	247.0	18410	.89
15516	100	Break-up	1313	1078	1.22	882	1090	.794	231.4	246.4	17990	.92
15820	100		1296	1027	1.26	917	1115	.763	233.4	248.2	18200	.89
15821	100		1294	1022	1.26	924	1118	.758	232.9	247.5	18070	.90
15825	100		1316	1052	1.25	890	1083	.787	233.0	247.8	18170	.90
		Average	1306	1050	1.24	902	1101	.777	232.5	247.2	18200	.90
15628	20		1059	895	1.18	1089	1264	.643	231.5	247.4	18280	.92
15721	20		1058	884	1.20	1102	1282	.635	231.3	247.4	18240	.93
15724	20		1070	866	1.24	1124	1380	.623	-	-	-	.90
15822	20		1036	856	1.21	1126	1313	.622	231.8	248.6	18120	.92
15826	20		1008	836	1.21	1132	1293	.628	229.4	246.4	17720	.92
15827	20		972	831	1.17	1149	1335	.609	231.6	249.0	18120	.91
		Average	1034	861	1.20	1120	1311	.627	231.1	247.8	18090	.92

The 100°F firings consistently showed a slight increase in pressure immediately before burnout (Fig. 9). This increase was probably caused by grain breakup when the propellant spokes became thin and were broken off by the gas stream. This type of behavior is expected to some extent with the Zeus geometry, but the pressure rise was not high enough to endanger the case. No performance loss could be detected. The breakup was less evident or non-existent in lower temperature firings, probably because of the greater strength of the propellant at the lower temperatures.

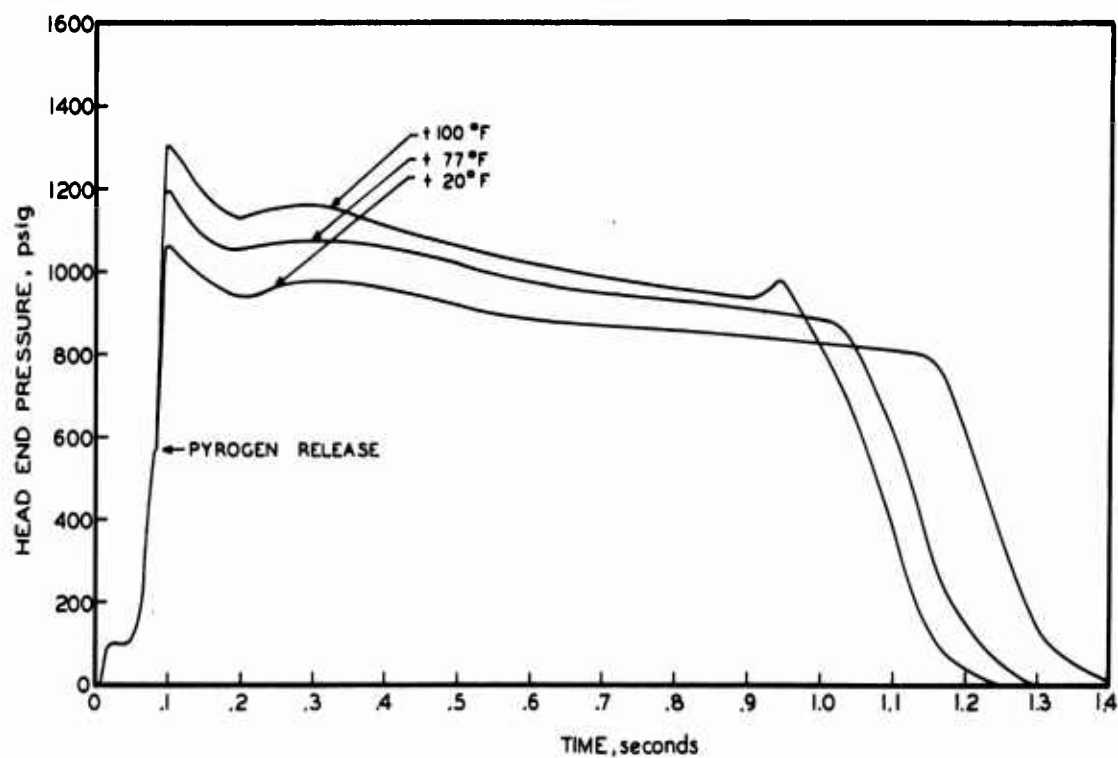


Fig 9 Pressure-time traces of 1/5-scale booster at various conditioning temperatures.

Two additional rounds were successfully fired at -2°F and 120°F to extend the data (Table XI).

Table XI  
Results of Firings of 8.5AS31 Motor at -2°F and 120°F  
Propellant Composition 178<sub>cf</sub>

Round	Temp. °F	$P_{max}$ psig	$P_b$ psig	$P_{max}/P_b$	$t_b$ msec	$t_a$ msec	$r_b$ in/sec	$\int P_b dt / \int P_{tot} dt$
16012	-2	921	769	1.22	1231	1411	.569	.92
16011	120	1345	1072	1.25	873	1198	.802	.87

Two rounds without known flaws behaved abnormally. Both were from propellant batch 178-1048; one was fired at 77°F, the other was fired at 100°F. The first (77°F) round exhibited a maximum pressure about 150 psi higher than normal. The shape of the pressure trace indicated a restrictor failure. The second round (100°F) showed a similar type pressure rise, but the pressure level was high enough to cause propellant breakup and subsequent case rupture. It was suspected that the bond between the propellant and restrictor was marginal and that the pyrogen blast may have caused a separation between the propellant and restrictor, causing a greater surface to be exposed to burning. Subsequent calculations have shown that the extra surface generated by complete restrictor failure will result in a burning pressure in the order of magnitude of 1800 psi. This pressure is sufficient to cause propellant breakup.

All motors were X-rayed before firing. Two motors in which flaws were indicated were fired to determine the effect of known flaws on the ballistic performance. The first motor X-rays revealed flaws at the head end of the slivers. Since this should not affect the first part of the pressure record, the motor was conditioned to 100°F and fired. As expected the first half of burning was normal,

but when the flaws were exposed to the flame, the pressure trace became rough, indicating minor propellant breakup. Examination of the expended case confirmed the X-ray analysis, showing premature burning at the head end of the slivers. Inspection of the second motor revealed either propellant or insulation cracks in the dome section of the motor. The cracks did not propagate during two cycles between  $-40^{\circ}\text{F}$  and  $120^{\circ}\text{F}$ , and were assumed to be in the insulation. During firing a burn-through occurred in the head where the cracks were located. Examination of the sectioned motor showed the flaws to be in the insulation as suspected. This was one of the first motors insulated with 42-RPD and the joints in the head end laminations were not overlapped as in the later motors. As a result only resin filled the small gaps between the edges of the laminations, providing inadequate insulation at those points and showing up as cracks in the X-rays. In both cases after careful X-ray examination and analysis, the performance of the motors was reasonably predicted.

To measure the effect of cycling between temperatures of  $-40^{\circ}\text{F}$  and  $120^{\circ}\text{F}$ , two rounds from each of the five demonstration batches were set aside. The first five rounds were subjected to two complete cycles of approximately 84 hours at each temperature extreme, and fired at  $77^{\circ}$  (Table XII). The remaining five are still being cycled.

During the preliminary evaluation phase of the program, twenty-four 1/5-scale motors were cast from 18 batches of propellant of which 23 were acceptable for ballistic firings. Thirty-nine additional 1/5-scale motors were cast from six batches of propellant and prepared for the demonstration phase of the program. Two were rejected, one due to poor quality propellant and the other because of a

short charge. Thirty motors have been fired over a temperature range of -2°F to 120°F; five of these after temperature cycling between -40°F and 120°F. There was only one failure. Five additional motors are still being temperature cycled and two have been prepared for acceleration flight testing. The overall yield of successful firings to date has been approximately 93% (52 out of 56).

Table XII  
Results of Firings of 8.5AS31 Motors After Cycling  
Propellant Composition 178<sub>cf</sub>  
Conditioned to 77°F Before Firing

Round	Comments	$P_{max}$ psig	$P_b$ psig	$P_{max/P_b}$	$t_b$ msec	$t_a$ msec	$r_b$ in/sec	$\int P_b dt / \int P_{tot} dt$
15783		1220	986	1.24	945	1153	.741	.90
15784	Head end Burnthrough (see text)	1240						
15959		1203	972	1.23	977	1160	.716	.91
15960		1235	986	1.25	965	1185	.725	.91
15961		1291	948	1.36	1000	1203	.700	.91

### 3.6 Calculated Performance of the Full-Scale Booster

Data obtained from the demonstration firings indicate that the full-scale booster loaded with plastisol Composition 178<sub>cf</sub> will meet the original requirements for the system. A comparison of the average 1/5-scale data and the corresponding predicted values for the full-scale motor is shown in Table XIII.

Table XIII  
Predicted Performance of the Full Scale Booster  
Compared to 1/5-Scale Data at 77°F

Scale	Prop. Weight lbm	$P_{max}$ psig	$\bar{P}_b$ psig	$t_b$ sec	$t_a$ sec	$I_m$ lbf-sec/lbm	$F^*_{1000}$ lbf-sec/lbm	$\int F dt$ lbf-sec
1/5	78.4	1194	981	0.978	1.167	232.9	248.3	18,240
Full	9775	1194	981	4.890	5.300	234.9 <sup>1</sup>	250.3 <sup>1</sup>	2,450,000

<sup>1</sup>Estimated values based on the fact that larger motor firings result in slightly higher specific impulses.

The target burning time of 960 milliseconds (4.8 seconds full-scale) was missed slightly in these tests. However, a slight change in oxidizer particle size can adjust the burning rate to the proper value.

Tail-off time, as evidenced by  $t_a$ , was considerably longer than desired. This deviation from the design value was the result of the preformed slivers not being scaled exactly and the inability to hold "scaled" tolerances on motor diameter. Actual performance in the full-scale motor should be substantially improved.

An average of 78.4 lb of propellant was loaded into the 1/5-scale booster. This corresponds to 9775 lb in the full-scale allowing for the off-scale slivers. The slightly higher density of Composition 178 over the present Zeus propellants accounts for most of the increased mass of propellant, the rest being obtained through the use of less case insulation. Based on the average delivered total impulse of 18,240  $lb_f$ -seconds of the 1/5-scale booster, a total impulse of over  $2.4 \times 10^6$   $lb_f$ -seconds was indicated for the full-scale motor, including an allowance for a slightly higher specific impulse in the larger motor.

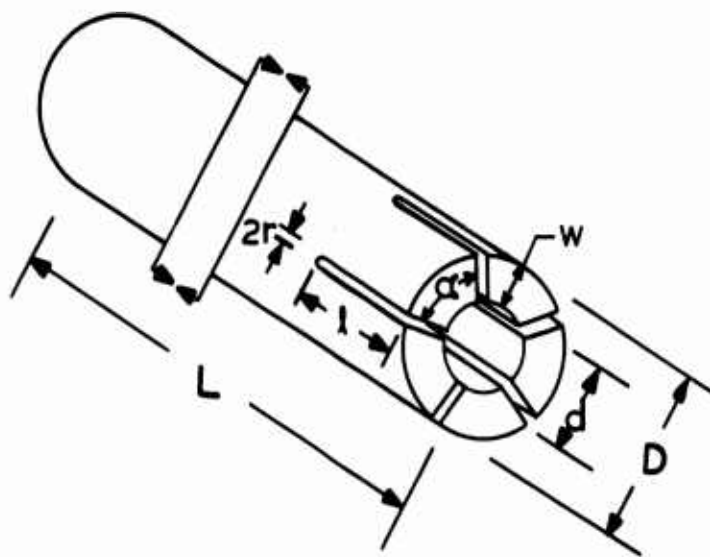
Using the present design of restrictor in the 1/5-scale motor would result in a maximum pressure ( $P_{max} + 3\sigma$  @ 100°F) of 1340 psi. This value may be adjusted if desired by a slight change in the restrictor.

### 3.7 Surveillance

To reduce the cost of this phase of the program a strain-scale motor was designed to replace the standard 1/5-scale motor

for storage. This motor was a standard 6 x 24 static test motor regularly used by this Division. The propellant has a cylindrical geometry six inches O.D. x three inches I.D. x 24 inches long. Five slots 3.82 inches long at one end of the grain make the burning nearly neutral. An insulating liner of approximately 0.03 inches of 42-RPD with a bonding liner of PL-1, the same as used in the 1/5-scale motors, was used. A layer of PR-46 restrictor was applied at the inside ends of the slots to provide long term compatibility data on the propellant-restrictor bond.

The calculated induced static strains in this configuration were designed to be about twice those expected in the 1/5-scale configuration to provide a reasonable safety factor. The 6SN24 propellant configuration is shown in Fig. 10.



$$d = 3.0 \text{ in.}$$

$$L = 24.0 \text{ in.} \quad r = 0.18 \text{ in.}$$

$$\alpha = 72^\circ \text{ in.} \quad l = 3.82 \text{ in.}$$

$$D = 6.0 \text{ in.} \quad w = 1.50 \text{ in.}$$

Fig. 10 Surveillance motor propellant configuration.

Seven batches of propellant were loaded into 130 surveillance motors. One hundred motors were placed in igloo storage. Ten of the balance, representing all seven batches of propellant, were fired to obtain base-line data for the lot (Table XIV). The balance of the motors were not used in this part of the program.

Table XIV  
6SN24 Surveillance Motor Baseline Data at 77°F  
Propellant Composition 178<sub>cb</sub>

Motor Number	P <sub>max</sub> psia	P <sub>b</sub> psia	t <sub>b</sub> msec	t <sub>a</sub> msec	r <sub>b</sub> in/sec	P <sub>max</sub> /P <sub>b</sub>	fP <sub>b</sub> dt/fP <sub>tot</sub> dt	I <sub>m</sub> lb-sec/lbm	F <sup>o</sup> <sub>1000</sub> lb-sec/lbm	Propellant Wt lbm	Batch
3	1097	1023	1877	1965	.778	1.07	.98	244.4	248.4	29.25	1045-7
4	1065	992	1914	2060	.763	1.07	.97	243.2	248.2	29.35	1047-20
7	1063	997	1945	2047	.751	1.07	.98	243.7	248.2	29.77	1041-15
38	1086	1015	1938	2012	.754	1.07	.98	244.6	248.6	29.78	1041-17
68	1115	1039	1869	1986	.781	1.07	.97	244.2	248.0	29.77	1044-8
8	1074	1016	1890	2024	.772	1.06	.97	244.0	248.3	29.79	1050-6
118	1074	1011	1928	2012	.757	1.06	.98	244.3	248.4	29.77	1049-15
5	1081	1012	1916	1986	.762	1.07	.98	244.4	248.5	29.58	1045-20
29	1086	1023	1903	1981	.767	1.06	.98	244.6	248.4	29.50	1039-6
12	1093	1025	1903	1985	.767	1.07	.98	244.8	248.6	29.82	1039-4
Average	1083	1015	1908	2006	.765	1.07	.98	244.2	248.4	29.64	
σ	16	14	25	31	.010	—	—	.5	.2	.21	
%σ	1.5	1.4	1.3	1.5	1.3	—	—	0.2	0.08	0.7	

Reproducibility of these motors was exceptionally good. Although the propellant was not trimmed to weight after casting, the measured impulse had a standard deviation of only 0.7%, indicating the success of processing quality control. When corrected values of specific impulse (F<sup>o</sup><sub>1000</sub>) were considered, a standard deviation of only 0.08% was obtained. Methods of calculations are presented in Appendix B.

### 3.8 Production Techniques

The ballistic quality of the propellant used in the Zeus program was routinely monitored by casting six 6C5-11.4 static test motors from each production batch of propellant. The burning rate of each round was corrected to a pressure of 1000 psi and to an integral

ratio of 0.97. The average of the six rounds provided a burning rate,  $R_b$ , for the batch. The overall standard deviation for the surveillance motor sample rounds was 3.3% and for the 1/5-scale sample rounds was 4.2% (Table XV). The lower average burning rates for the 1/5-scale samples are required to obtain the proper burning rate of 0.73 in/sec in the 1/5-scale configuration. Burning rates always appeared higher in the 1/5-scale configuration than in the 6C5-11.4 test motors for a given propellant composition. Composition 178<sub>cf</sub> resulted in the proper burning rate and burning time in the 1/5-scale motor.

Table XV

Burning Rates for Production Batches of  
Propellant in 6C5-11.4 Sample Motors

<u>Surveillance Batch</u>		<u>1/5-Scale Batch</u>	
<u>Batch</u>	<u>Burning Rate in/sec.</u>	<u>Batch</u>	<u>Burning Rate in/sec.</u>
178 <sub>cb</sub> -1039 <sup>1</sup>	0.742	178 <sub>cf</sub> -1042 <sup>1</sup>	0.666
-1041	0.728	-1046	0.649
-1044	0.747	-1048	0.649
-1045	0.757	-1052	0.639
-1047	0.728	-1053	0.638
-1049	0.728	-1055	0.633
-1050	0.743		

<sup>1</sup>The difference in burning rate in the two samples is due to the difference in perchlorate grind as designated by the subscripts cb and cf.

### 3.9 Logistics

Only one ingredient of plastisol propellant may offer any logistics problem, and that does not appear to be very serious. The

fluid ball powder which is produced by Olin-Mathieson Chemical Company is presently being made in their pilot plant facilities. The current capacity of their pilot plant is 25,000 to 30,000 lb/month of Type B fluid ball powder. According to Olin-Mathieson this capacity could be doubled in three to six months if necessary. In addition, if requirements demanded, their large plant facilities could be modified in three to six months to provide a capacity of 250,000 to 300,000 lb/month. This corresponds to about 2.5 million pounds of propellant per month or over 100 complete missiles per month, assuming an 80% production efficiency.

Triethylene glycol dinitrate (TEGDN), the plasticizer, has been obtained by this Division on competitive bids from three suppliers, Hercules Powder Company, du Pont Company, and Propellex Chemical Company. All suppliers have produced satisfactory TEGDN. Since this material is made with the same equipment used for making nitroglycerin, adequate facilities are already in existence throughout the country. There should be no supply problem with TEGDN.

ALCOA 140 aluminum powder has been used throughout this program because it has the smallest particle size available, is the cheapest, and gives the lowest propellant viscosity. Although this powder is currently in good supply, it is not considered commercially available. To eliminate any possible logistics problem with aluminum powder, several other grades were considered as possible substitutes for ALCOA 140. Several batches of Composition 112<sub>cd</sub> propellant were made with the various grades of aluminum powder. The results of the evaluation are shown in Table XVI.

Table XVI  
Effect of Aluminum Powder on Properties of 112<sub>cd</sub> Propellant

Aluminum Powder Mfg.	Type	Size <sup>1</sup> Microns	Batch Viscosity <sup>2</sup> cp	Charpy Brittle Point °F	Elongation %			Tensile Strength psi			F <sub>1000</sub> lbf-sec/lbm	F <sub>b</sub> in/sec	Cost/lb \$
					-40°F	77°F	140°F	-40°F	77°F	140°F			
Alcoa	140	7	5,600	-15	10	19	21	900	56	43	244.9	0.708	0.40
Alcoa	123	33	13,600	-10	11	19	21	574	57	41	244.2	0.687	
Alcoa	146	13	6,400	-10	11	16	20	543	57	41	245.0	0.687	.85
Alcoa	1230	27	10,800	-15	11	18	23	615	59	45	244.4	0.691	
Reynolds	1-131	10	5,600	-10	11	21	21	632	58	45	244.9	0.713	.90
Reynolds	1-511	29	12,000	-10	13	19	20	590	60	44	244.5	0.693	
Valley	H-10	10	8,000	-10	14	20	19	448	58	46	245.0	0.676	

<sup>1</sup>By Micromerograph

<sup>2</sup>By Brookfield; T-B Spindle at 5 rpm

1. Reynolds 1-131 is an adequate substitute for ALCOA 140 in all respects.
2. ALCOA 146, with slight oxidizer particle size reduction, is also a suitable substitute.
3. ALCOA 123, ALCOA 1230, and Reynolds 1-511, with slight oxidizer particle size reduction, are also suitable substitutes, provided adequate allowance is made in the processing to accommodate the increased viscosity that these powders cause.
4. Valley H-10 is suitable, subject to the same restrictions as those in 3, but it would require a greater oxidizer particle size shift than any of the other powders.

Cost data are given only for the most promising substitute powders. The characteristic which makes ALCOA 140 cheaper than the others is the same one which makes it unavailable commercially; it is a by-product.

# CONFIDENTIAL

## APPENDIX A

### Establishment of Strain Capability of Plastisol Propellants

A propellant needs both adequate tensile strength and elongation to be of value in a missile system such as Nike-Zeus. To improve the utility of a propellant in a missile system, two approaches may be used: increase the physical properties or reduce the driving force imposed on the physical properties. Since Composition 112 was selected as the propellant for the initial phase of the investigation, the physical properties had already been established. Therefore, a reduction in the driving force was investigated. The change to Composition 178 later in the program resulted in another set of fixed physical properties, slightly lower than those of Composition 112. The principal driving forces are the volumetric curing shrinkage and the thermal strains due to cooling. By reducing the cure temperature of the propellant, the strains due to cooling can be reduced. To confirm this, two 2C1.0-7.5 strain evaluation cylinders were cast. One was cured at 117°F and the other at 100°F. Measurements of maximum hoop strain were made at eight different temperatures. The result was an approximate 17°F lateral shift of the strain-temperature curve as shown in Fig. A-1, the lower strains being associated with the lower cure temperature. Curing shrinkage remained virtually constant within the limits of measurement at the cure temperatures investigated. Based on this information a cure temperature of 105°F was selected, because of the difficulty of maintaining a controlled 100°F cure during the summer months.

CONFIDENTIAL

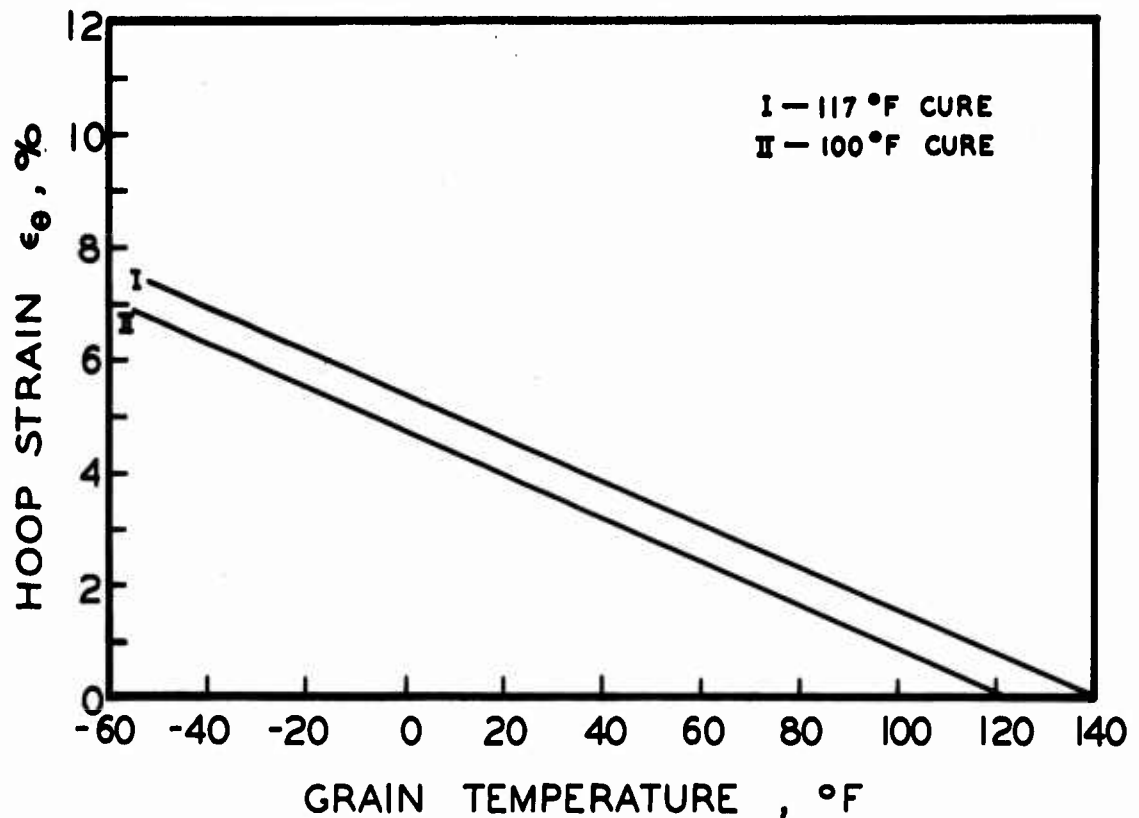


Fig. A-1 Effect of cure temperature on induced strain.

The low temperature strain evaluation program normally uses either 2 x 7.5 or 2 x 12 strain evaluation cylinders with a judiciously chosen set of cylindrical mandrels to provide a preselected hoop strain at various temperatures. The propellant was subjected to a stepwise low temperature conditioning to failure. A strain-temperature plot was made for each web thickness and the graph was separated into three zones, one where failure always occurs, one where failure sometimes occurs, and one where no failure occurs (Fig. A-2). The boundary between the intermediate and no failure zones is a conservative value of hoop strain capability of the propellant.

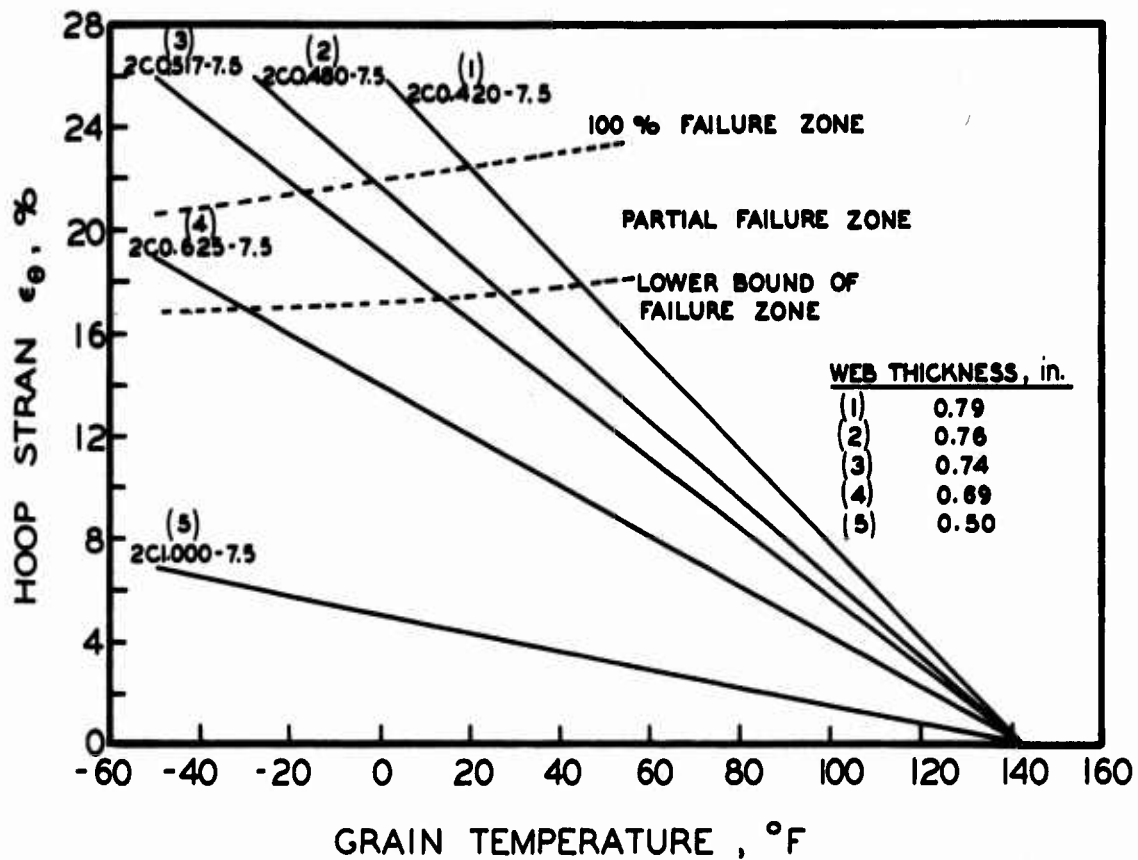


Fig. A-2 Strain capability of Composition 112cb as a function of web thickness.

The geometries and parameters for the test program with Composition 112 are listed in Table A-I.

A similar set of tests was conducted on three higher density propellants, Composition 176, 177, and 178. The geometries and parameters for this program are listed in Table A-II.

Table A-I

Evaluation Cylinder Geometries and Parameters

<u>Geometry</u>	<u><math>\omega^*</math></u>	<u><math>K_{\omega^*}</math></u>	<u>f</u>	<u><math>K_{\omega^*}</math> (eff.)</u>
2C1.000-7.5	0.250	1.500	1.00	1.500
3C1.000-22	0.327	3.677	1.00	3.677
2C0.625-7.5	0.344	4.636	0.90	4.172
2C0.517-7.5	0.370	6.896	0.84	5.793
3.75C1.000-24	0.362	6.064	0.98	5.943
2C0.480-7.5	0.380	8.181	0.81	6.627
2C0.420-7.5	0.395	10.838	0.72	7.803
2C0.365-7.5	0.408	14.268	0.68	9.702

where  $\omega^*$  = reduced web

$$K_{\omega^*} = \text{geometry normalizing parameter} = \frac{2\omega^*(1-\omega^*)}{(1-2\omega^*)^2}$$

f = finite length correction term

$$K_{\omega^*} \text{ (eff.)} = K_{\omega^*} f.$$

Table A-II

Evaluation Cylinder Geometries and Parameters

<u>Geometry</u>	<u><math>\omega^*</math></u>	<u><math>K_{\omega^*}</math></u>	<u>f</u>	<u><math>K_{\omega^*}</math> (eff.)</u>
2C1.000-7.5	0.250	1.500	1.00	1.500
2C0.750-7.5	0.312	3.037	0.96	2.916
2C0.646-7.5	0.338	4.263	0.92	3.922
2C0.518-7.5	0.370	6.896	0.84	5.793
2C0.502-7.5	0.375	7.500	0.83	6.225
2C0.480-7.5	0.380	8.181	0.81	6.627
2C0.420-7.5	0.395	10.838	0.73	7.912
2C0.365-7.5	0.408	14.268	0.68	9.702
2C0.306-7.5	0.423	20.583	0.56	11.526

The lower bound curves for these compositions are shown on Fig. A-3 along with a curve for Composition 112. If the values shown in Fig. A-3 are normalized for composition, since varying amounts of binder in the propellant affect the driving force leading to induced hoop strain, the curves in Fig. A-4 will result, giving a more realistic indication of the merit of each composition in a loaded motor. Normalization is accomplished by dividing the strain value by the volume fraction of the binder, where the binder is defined as the ball powder plus the plasticizer. The effect of small changes of oxidizer particle size on the strain capability of a propellant was insignificant.

#### Scale Booster Strain Requirements

The charge diameter of the 1/5 scale motor was 8.5-inches and the propellant web was 0.70-inches resulting in a reduced web,  $\omega^*$ , of 0.082. The geometry normalizing factor  $K_{\omega^*}$  for a cylindrical charge of this reduced web is 0.215. Using a strain concentration factor of 2.6, which is a calculated estimate comparing the strains in a complex wagon wheel perforation to a cylindrical perforation, an effective  $K_{\omega^*}$  was determined to be 0.559. No correction was included for finite length. A cylindrical grain with a reduced web of 0.156 would also have this value of  $K_{\omega^*}$ .

In the 6-inch strain-scale motors (6SN24) used for the surveillance program, a strain of approximately twice that expected in the 1/5-scale motor was selected to include a safety factor. This implies a  $K_{\omega^*}$  of 1.118 and a corresponding reduced web ( $\omega^*$ ) of 0.237 (web = 1.42 in.). For convenience a three-inch diameter mandrel (instead of a calculated 3.12 in. diameter) was chosen, resulting in an actual web of 1.48". Ninety percent of the infinite cylinder strain can

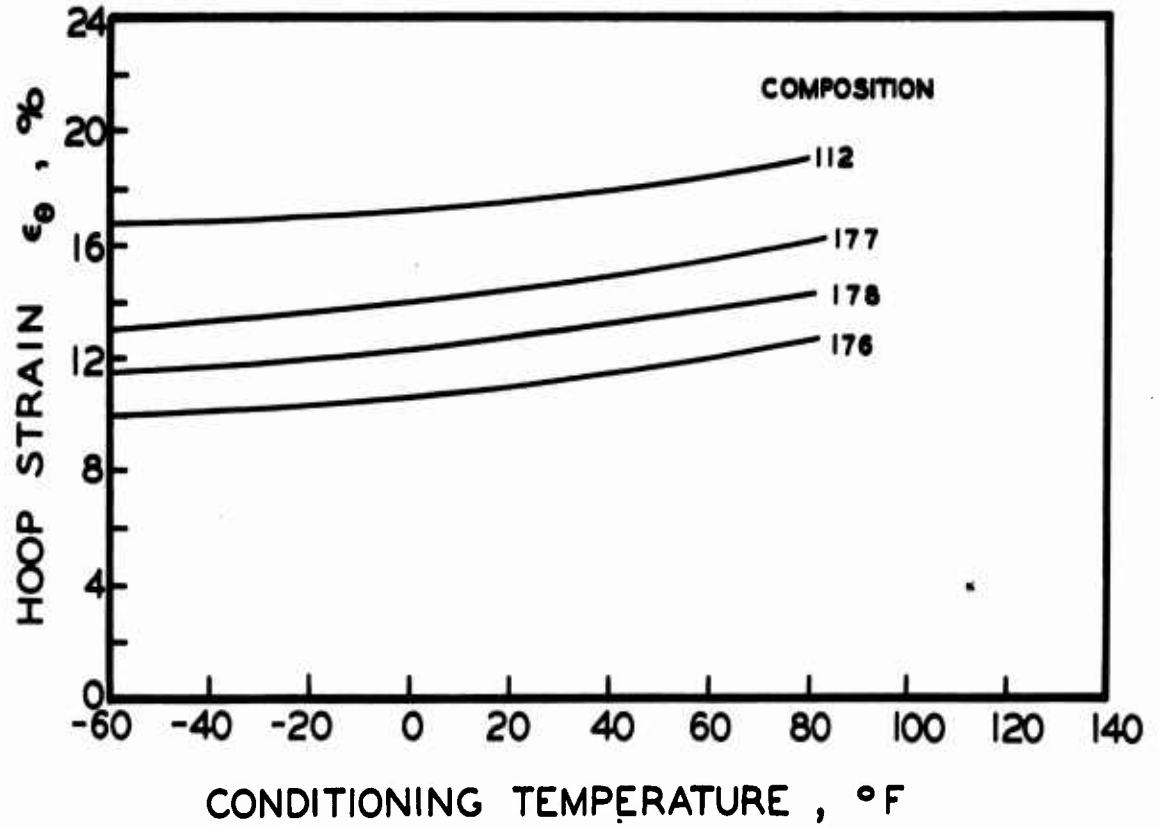


Fig. A-3 Strain capability vs. conditioning temperature for various propellant compositions.

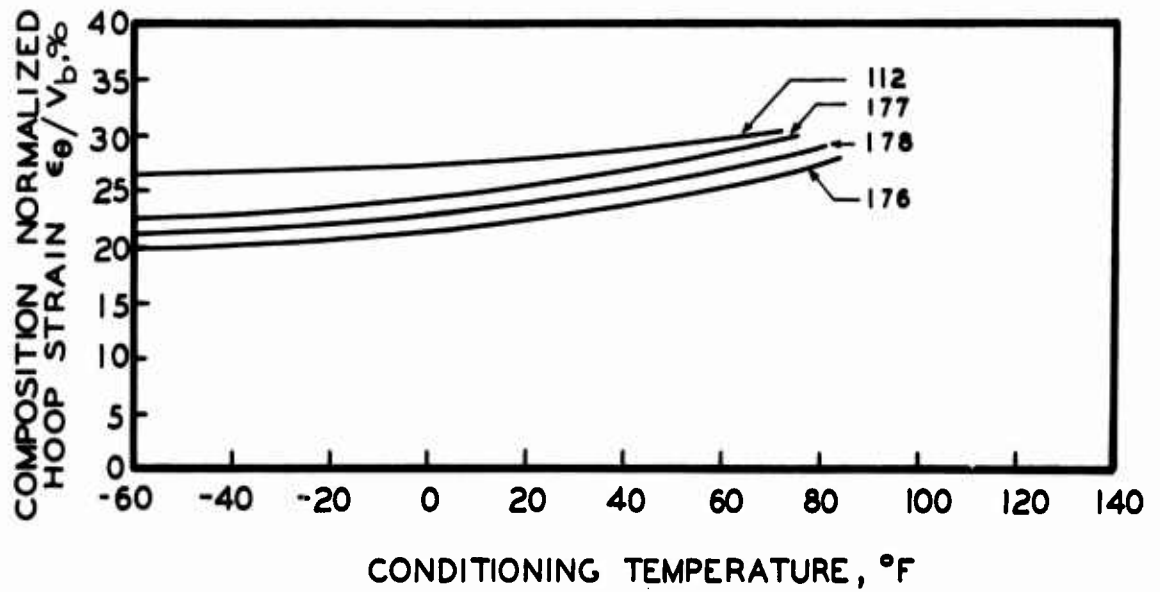


Fig. A-4 Strain capability vs. conditioning temperature for various propellants normalized for compositions.

be expected within four inches of the unslotted end of a 6SN24 motor case. Using reduced hoop strain (hoop strain/ $K_{\omega^*}$ ) versus temperature data for Compositions 112 and 178 (105°F cure), hoop strain requirements for the surveillance and 1/5-scale booster configurations are shown in Fig. A-5.

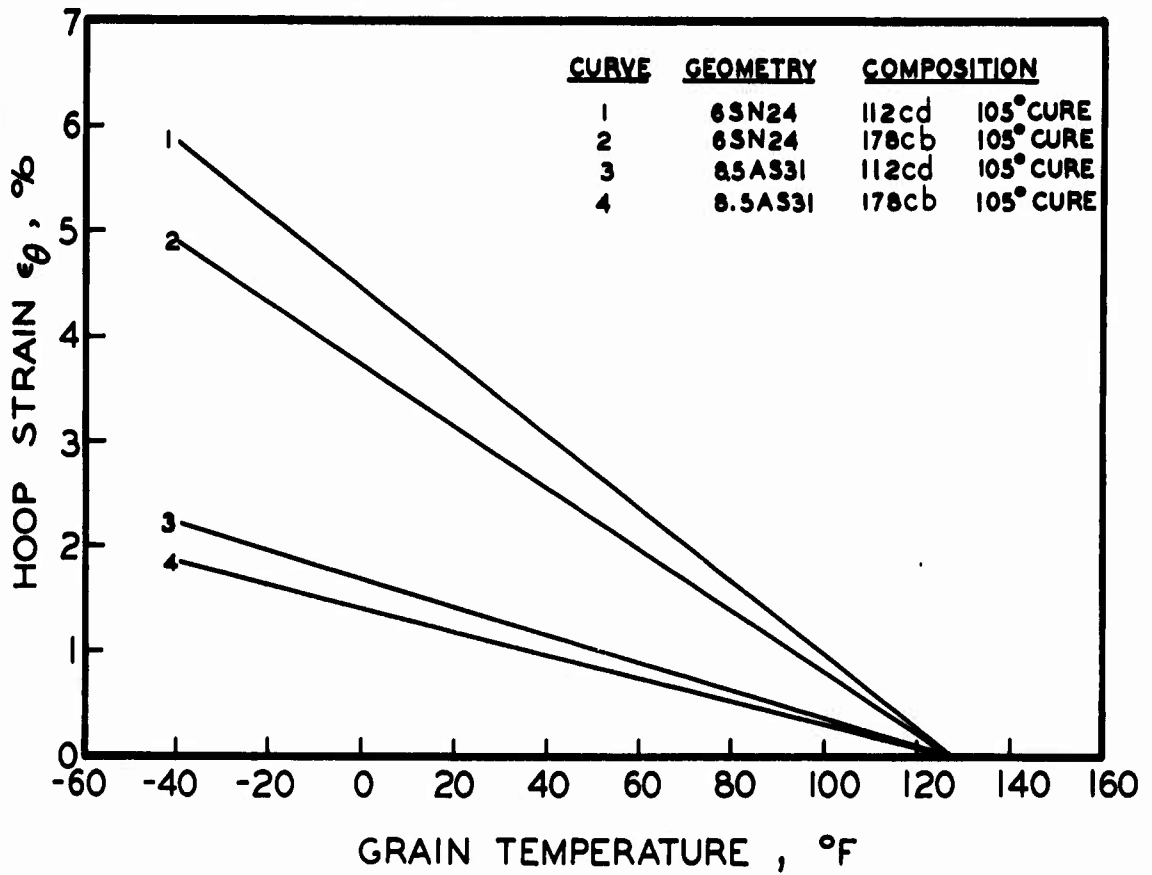


Fig. A-5 Hoop strain requirements for the 6SN24 and 8.5AS31 configurations.

Effect of Humidity on Physical Properties of Plastisol Propellants

Humidity has a significant effect on the physical properties of plastisol propellants. As the moisture content of the propellant was increased, the tensile strength decreased, and the strain at maximum engineering stress increased. The effect on strain was much less marked than the effect on tensile strength except at 100% relative humidity where the strains increased to very high values.

Both Compositions 112 and 178 have been investigated, and the effect of humidity on tensile strength appeared to be nearly a universal function when the tensile strengths were related to the zero humidity condition (Fig. A-6). A binder composition, consisting of a 1:1 ratio of ball powder/TEGDN, exhibited a similar behavior when conditioned in a manner similar to the propellant compositions, implying that the binder alone is responsible for the observed behavior. In addition, the effect of humidity on physical properties also appeared to be a reversible process.

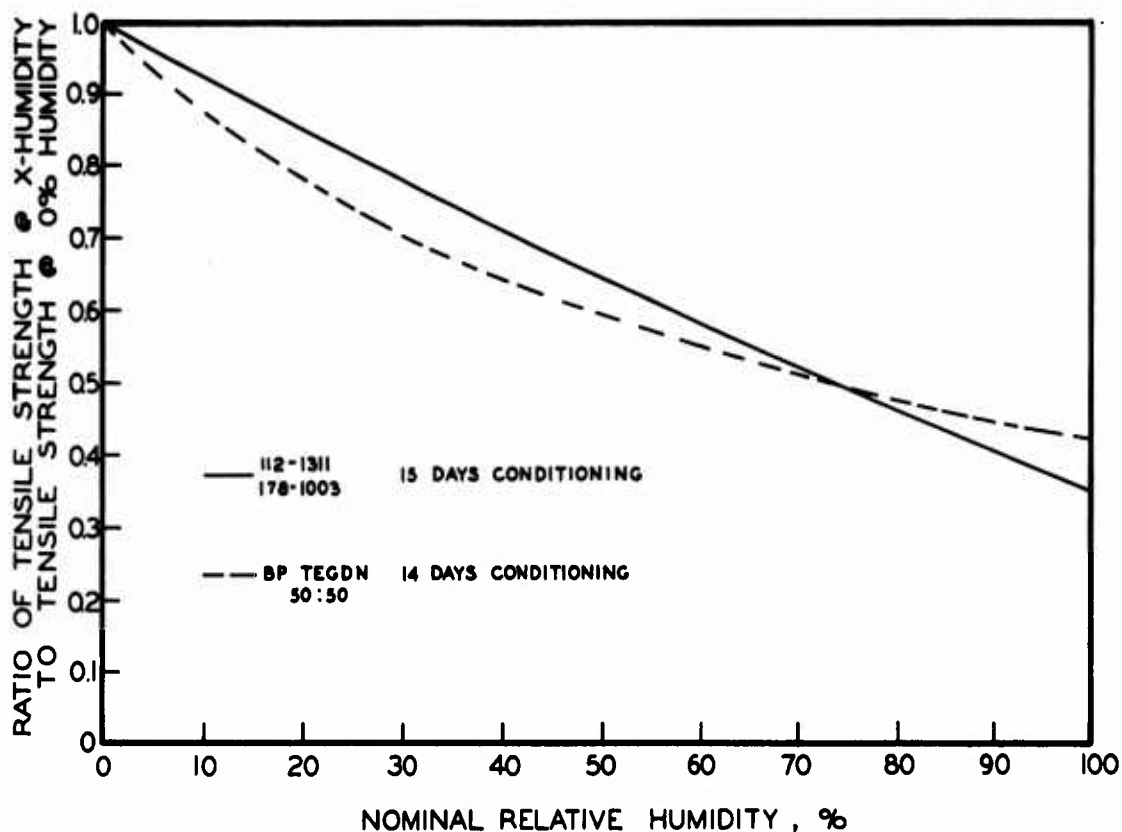


Fig. A-6 Effect of humidity on tensile strength of compositions 112 and 178.

Because of the humidity effect, all test samples were conditioned to a standard relative humidity (33-1/3%) before testing.

# CONFIDENTIAL

## APPENDIX B

### Methods of Computation for Surveillance Motors

#### I. Definition of Calculated Ballistic Quantities

A sketch of typical pressure-time and thrust-time traces with measurements indicated is shown in Fig. B-1. There are no timing marks shown. Oscillations on the thrust trace are smoothed as indicated by the dotted line for the purpose of integrating the area under the curve. This however is done only when the digital data are not obtained or are unsatisfactory. The following formulas describe the calculations made from the static test records and from the digital instrumentation. The latter supplies total thrust and pressure integrals, as well as integrals of pressure over burning time and over action time.

PF(psi/in.) = pressure factor =

$$\frac{\text{calibration value of step} \times \text{value of pressure gauge (psi)}}{\text{height of step (in.)} \times \text{gauge calibration factor}}$$

interpolation between two calibration steps is as follows

(see Fig. B-1):

$$PF = \frac{PF_3(d_4 - d_3) + PF_4(d_e - d_3)}{d_4 - d_3}$$

TF(lbf/in.) = thrust factor - obtained in same way as PF.

tF(msec/in.) = time factor =

$$\frac{\left[ \frac{\text{a given number of timing marks (counts)} \times 1000}{\text{total length of timing marks (in.)}} \right]}{\text{rate at which timing marks are produced (counts/sec)}}$$

CONFIDENTIAL

$$\text{Ignition Delay (msec)} = \text{ignition delay (in.)} \times \text{tF (msec/in.)}$$

$$t_b \text{ (msec)} = \text{burning time} = t_b \text{ (in.)} \times \text{tF (msec/in.)}$$

$$t_a \text{ (msec)} = \text{action time} = t_a \text{ (in.)} \times \text{tF (msec/in.)}$$

$$\text{or } t_{ap} \text{ (msec)} = t_{ap} \text{ (in.)} \times \text{tF (msec/in.)}$$

$$\bar{r}_b \text{ (in./sec)} = \text{average burning rate over burning time} =$$

$$\frac{\text{web(in.)} \times 1000}{t_b \text{ (msec)}}$$

$$\bar{r}_a \text{ (in./sec)} = \text{average burning rate over action time} =$$

$$\frac{\text{web(in.)} \times 1000}{t_a \text{ (msec)}}$$

$$K_m = \frac{S}{A_{tm}}, \text{ where } S_m \text{ is an integral average surface area and}$$

$A_{tm}$  is the arithmetic average of throat area before and after firing. Throat diameter after firing is measured before any accumulated deposit is removed.

$$n = \text{slope of } \log \bar{r}_b \text{ versus } \log \bar{P}_b \text{ line}$$

$$P_{ig} \text{ (psia)} = \text{ignition pressure} = P_{ig} \text{ (in.)} \times \text{PF (psi/in.)} + 14.4^1$$

$$P_{max} \text{ (psia)} = \text{maximum pressure} = P_{max} \text{ (in.)} \times \text{PF (psi/in.)} + 14.4$$

---

<sup>1</sup>Average atmospheric pressure at geographical location of test facility.

$\bar{P}_b$  (psia) = average pressure over burning time =

$$\frac{\int_{t_b} P dt(\text{in.}^2) \times tF(\text{msec/in.}) \times PF(\text{psi/in.})}{t_b (\text{msec})} + 14.4$$

$\bar{P}_a$  (psia) = average pressure over action time =

$$\frac{\int_{t_a} P dt(\text{in.}^2) \times tF(\text{msec/in.}) \times PF(\text{psi/in.})}{t_{ap} (\text{msec})} + 14.4$$

$\pi_k$  = temperature coefficient of pressure at constant K =

$$\frac{P_2 - P_1}{1/2(P_1 + P_2)} \times \frac{100}{T_2 - T_1}, \text{ where } P_1 \text{ is average pressure}$$

over burning time at temperature  $T_1$  and  $P_2$  is average pressure over burning time at temperature  $T_2$ .

$\int Pdt$  (psia-sec) = total pressure-time integral =

$$\frac{\int P_{\text{total}} dt(\text{in.}^2) \times tF(\text{msec/in.}) \times PF(\text{psi/in.})}{1000} + 14.4 (\text{psi}) \times$$

length of pressure trace (sec)

$F_{\text{max}}$  (lbf) = maximum thrust =  $F_{\text{max}}$  (in.)  $\times$  TF(lbf/in.)

$\bar{F}_a$  (lbf) = average thrust over action time =

$$\frac{\int_{t_a} F dt (\text{in.}^2) \times tF(\text{msec/in.}) \times TF(\text{lbf/in.})}{t_a (\text{msec})}$$

$\int_{t_a} F dt(\text{lb-sec}) = \text{thrust-time integral} =$

$$\frac{\int_{t_a} F dt(\text{in.}^2) \times tF(\text{msec/in.}) \times TF(\text{lb/in.})}{1000}$$

$$I_m (\text{lb-sec/lbm}) = \text{measured impulse} = \frac{\int_{t_a} F dt(\text{lb-sec})}{\text{charge wt. (lbm)}}$$

Charge weight is the difference between weight before firing (before inhibitor is applied) and weight after firing.

$C_D (\text{lbm/lb-sec}) = \text{discharge coefficient} =$

$$\frac{\text{charge wt. (lbm)}}{\frac{\text{mean area of nozzle throat (in.}^2)}{\int P dt (\text{psi-sec})}}$$

$$\dot{m} (\text{lbm/sec}) = \text{mass discharge} = \frac{\text{charge wt. (lbm)} \times 1000}{t_a (\text{msec})}$$

$$C_F = \text{thrust coefficient} = I_m (\text{lb-sec/lbm}) \times C_D (\text{lbm/lb-sec})$$

$$c^* = (\text{ft/sec}) = \text{characteristic exhaust velocity} = \frac{g(\text{ft/sec}^2)}{C_D (\text{lbm/lb-sec})}$$

$F^{\circ}_{1000}$  = specific impulse corrected to 1000 psia pressure, optimum expansion, and  $0^\circ$  exit cone half angle. The correction procedure is as follows:

$$F^{\circ}_{1000} = I_m \left( \frac{C_F(\text{std})}{C_F(\text{test})} \right)$$

$C_F(\text{std})$  is a function only of the specific heat ratio ( $\gamma$ ) and is taken from a table of such values.

$C_F(\text{test})$  can be found from the relationship

$$C_F(\text{test}) = C_F(\text{vac}) - \epsilon \left( \frac{P_{\text{amb}}}{\bar{P}_a} \right)$$

where  $C_F(\text{vac})$  is a function of  $\gamma$  and  $\epsilon$  (expansion ratio,  $A_e/A_t$ ), and is obtained from a Table;  $P_{\text{amb}}$  is the average barometric pressure for the range location, namely 14.4 psi at Huntsville, Alabama; and  $\bar{P}_a$  is the average pressure over the action time.

$I_{\text{sps}} = F^{\circ}_{1000}$  when the following conditions have been met:

- (a) The trace must be neutral within the limits

$$0.90 \leq \frac{P}{\bar{P}_b} \leq 1.10$$

over the equilibrium portion of the trace.

- (b)  $800 \leq \bar{P}_a \leq 1200$ .

- (c) The tail-off portion of the trace is limited by the following:

$$t_b \geq 0.87 t_a$$

$$\frac{\int P_{t_b} dt}{\int P_{\text{total}} dt} \geq 0.95.$$

$I^{\circ}_{1000} = I_{sps} = F^{\circ}_{1000}$  when the following conditions have been met:

(a)  $900 \leq \bar{P}_a \leq 1100$

(b)  $\frac{\int P_{t_b} dt}{\int P_{total} dt} \geq 0.95$

(c)  $8 \leq \frac{A_e}{A_t} \leq 11$

(d) Records must be obtained from a 6 x 11.4 in. static test motor with 5-in. cylindrical perforation.

$C_{DO}$  = discharge coefficient corrected for pressure drop along the length of the grain =  $C_D (P_h / P_c)$ ,

where  $P_h$  is the head end pressure and  $P_c$  is the stagnation pressure at the entrance to the converging section of the nozzle.

Calculate  $J_o$  (initial ratio of throat area to port area) and from Fig. B-2 find the corresponding mach number ( $M_{Lo}$ ). Calculate  $J_f$  (final J) and from Fig. B-2 find  $M_{Lf}$ . Calculate an average  $M_L$  by means of the following formula.

$$M_L = 0.03 (M_{Lo}^2 - M_{Lf}^2) + 0.5 (M_{Lo} + M_{Lf}),$$

where  $M_L$  is the mach number at the end of the grain, and the subscripts "o" and "f" again refer to initial and final conditions, respectively.

From Fig. B-3 find the value of  $P_h / P_c$  corresponding to  $M_L$  and substitute in the formula for  $C_{DO}$ .

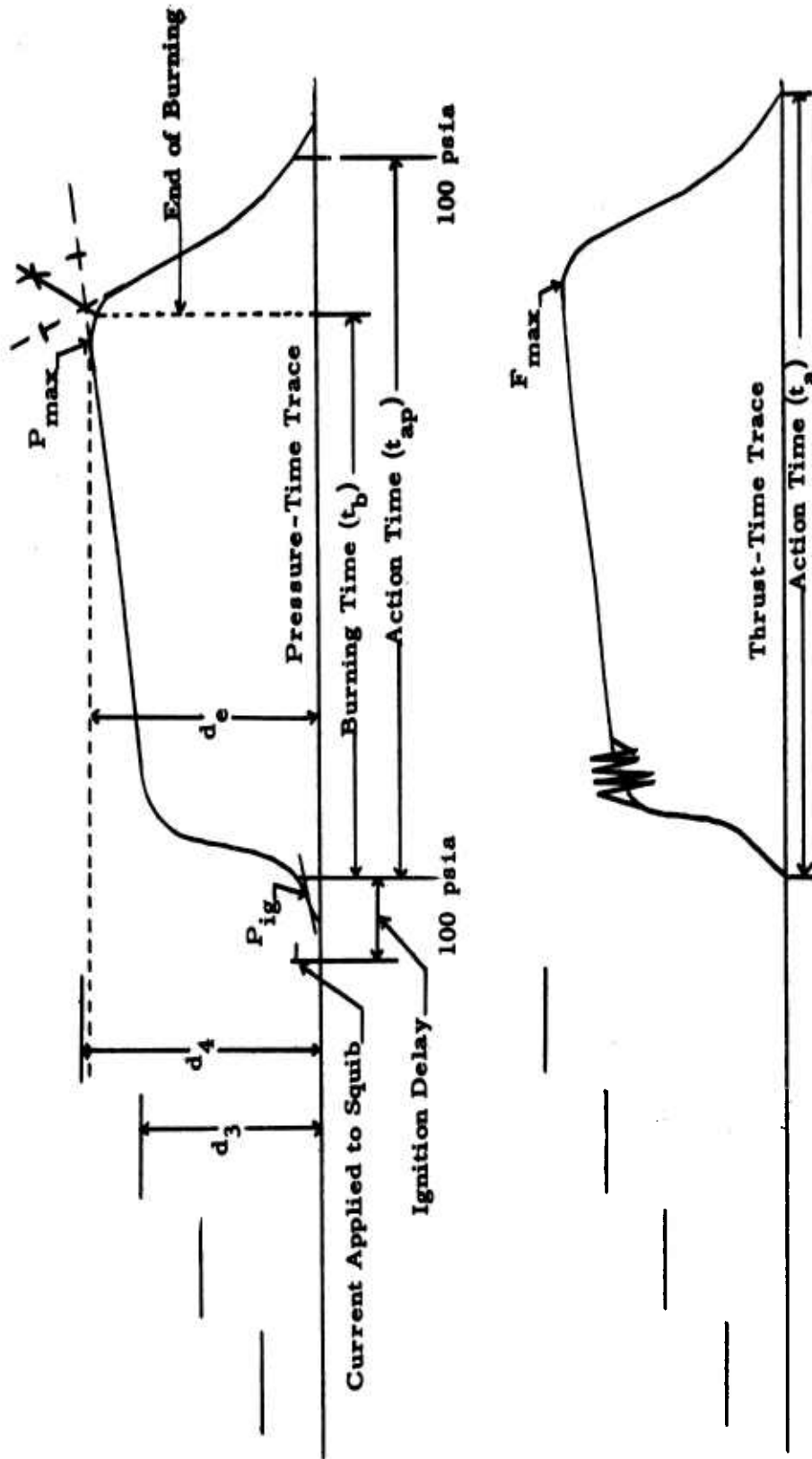


Fig. B-1 Typical pressure-time and thrust-time traces.

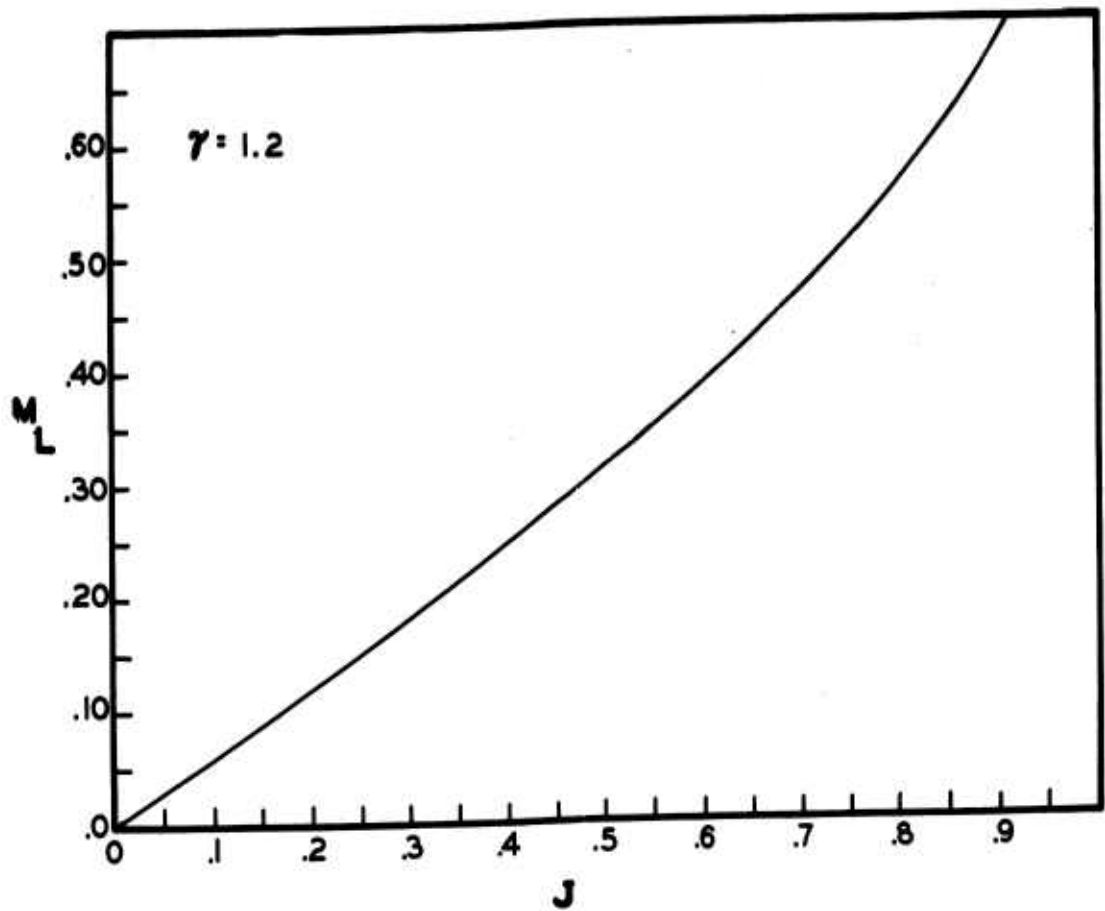


Fig. B-2 Mach Number as a function of  $J$  for  $\gamma=1.2$

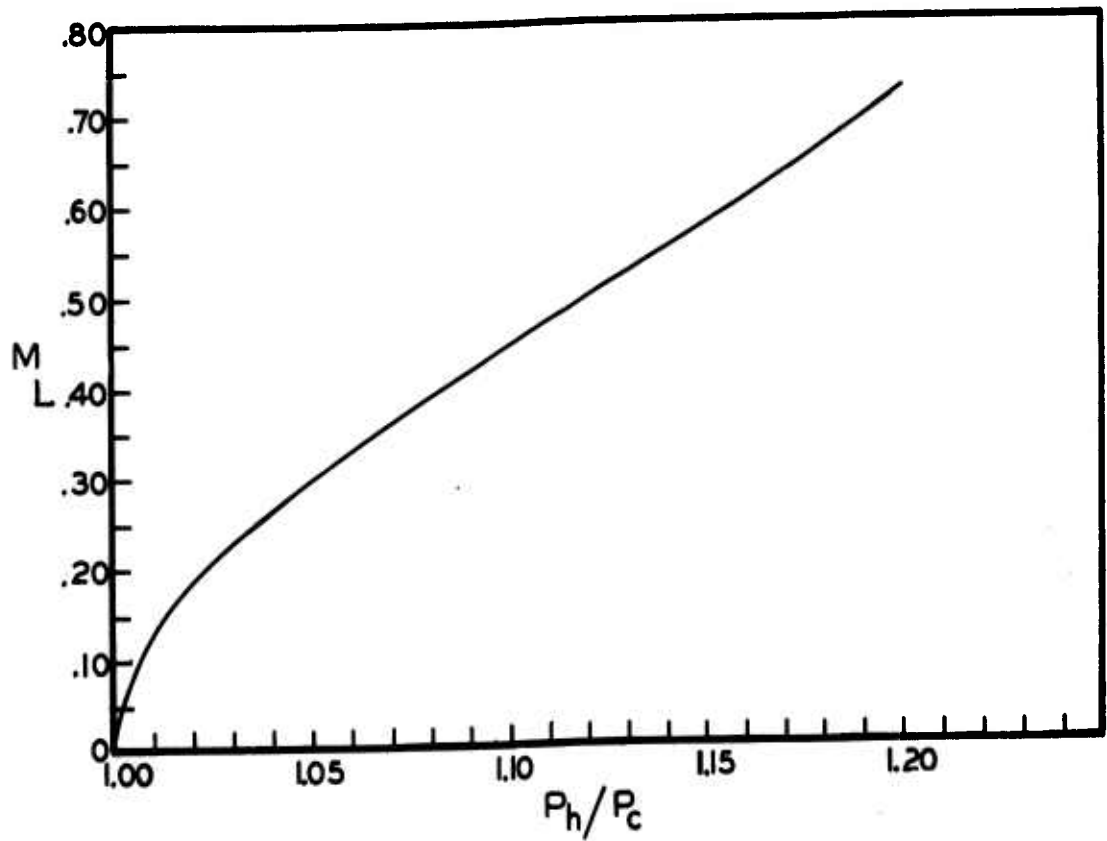


Fig. B-3  $M_L$  as a function of  $P_h/P_c$ .

Initial distribution of this report was made  
in accordance with the Joint Army-Navy-  
Air Force mailing lists for Solid Propellant  
and Liquid Propellant technical information  
plus approved supplements

UNCLASSIFIED

UNCLASSIFIED